ACS SENSORS

pubs.acs.org/acssensors

Review

Antifouling Strategies for Electrochemical Biosensing: Mechanisms and Performance toward Point of Care Based Diagnostic Applications

Matthew J. Russo, Mingyu Han, Pauline E. Desroches, Clayton S. Manasa, Jessair Dennaoui, Anita F. Quigley, Robert M. I. Kapsa, Simon E. Moulton, Rosanne M. Guijt, George W. Greene,* and Saimon Moraes Silva*

Cite This: *ACS Sens.* 2021, 6, 1482–1507

Read Online

ACCESS | Metrics & More | Article Recommendations

ABSTRACT: Although there exist numerous established laboratory-based technologies for sample diagnostics and analyte detection, many medical and forensic science applications require point of care based platforms for rapid on-the-spot sample analysis. Electrochemical biosensors provide a promising avenue for such applications due to the portability and functional simplicity of the technology. However, the ability to develop such platforms with the high sensitivity and selectivity required for analysis of low analyte concentrations in complex biological samples remains a paramount issue in the field of biosensing. Nonspecific adsorption, or fouling, at the electrode interface via the innumerable biomolecules present in these sample types (i.e., serum, urine, blood/plasma, and saliva) can drastically obstruct electrochemical performance, increasing background "noise" and diminishing both the electrochemical signal magnitude and specificity of the biosensor. Consequently, this review aims to discuss strategies and concepts used throughout the literature to prevent electrode surface fouling in biosensors and to communicate the nature of the antifouling mechanisms by which they operate. Evaluation of each antifouling strategy is focused primarily on the fabrication method, experimental technique, sample composition, and electrochemical performance of each technology highlighting the overall feasibility of the platform for point of care based diagnostic/detection applications.

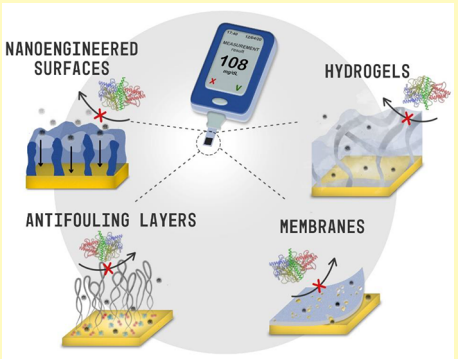

KEYWORDS: *biosensors, electrochemical detection, point of care diagnostics, interfaces, antifouling, nonspecific adsorption, biomolecules, nanoengineered surfaces, membranes, hydrogels, commercialization*

Moving medical and forensic diagnostics out of the analytical laboratory and into the field demands technologies that provide rapid results and can be used with minimal training, sample processing, or handling. However, a critical and enduring issue regarding the development and performance of biosensing technologies is biofouling, which is a result of nonspecific adsorption of proteins and other biological molecules present in biological media (i.e., blood, saliva, and urine) to the sensor surface. Surface fouling can result in the loss of specificity, device contamination, and overall electrode passivation, all of which can significantly contribute to device failure. In addition, complex biological media often possess extremely low target analyte concentrations with respect to other background species within the sample, where even minor degradation in signal intensity or increase in background noise can prove disastrous with respect to device accuracy and function.[1] As a result, research in the field of electrochemical biosensing has been focused on the investigation of different antifouling strategies for electrode surfaces in order to overcome the issue of biofouling, including some reviews which highlight antifouling strategies using biocompatible or biological materials.[2,3] In order to develop an effective antifouling surface, it is important to understand the interactions between the surface and biological molecules, and the resulting impact they have on the electrochemical signal response. The most effective strategies should aim to balance the trade-off between the antifouling properties and the electrochemical detection capabilities of the biosensor surface. There are many studies investigating antifouling strategies for electrochemical biosensors; however, this review will position the focus of its discussion on only the promising strategies for

Received: February 22, 2021
Accepted: March 16, 2021
Published: March 25, 2021

https://doi.org/10.1021/acssensors.1c00390
ACS Sens. 2021, 6, 1482–1507

point of care (POC) based diagnostic/detection applications, where analyte detection is performed in situ using complex media in direct contact with the sensor surface. Analysis will include the antifouling strategies used and the mechanisms by which they operate, while also highlighting the fabrication and synthetic techniques used for a given strategy to evaluate the commercial feasibility of the platform.

POC diagnostics are needed in a number of clinical areas, including hospitals, home monitoring, and rapid health screening. It is also increasingly important in illicit drug detection, as the detrimental effects of substance abuse toward the overall health of a patient leak into many different aspects of society including drivers, athletes, social environments, and the workplace.[4−6] POC-based electrochemical biosensors can provide a platform for many of these diagnostic applications, including those required by nurses, paramedics, and police officers. To develop electrochemical biosensing technology for these applications, the POC platform must be simple to use, applicable to rapid field-based sample analysis (i.e., out of the laboratory) and commercially viable in terms of fabrication and cost and must exhibit accurate and reliable results for complex biological samples. As a result, we will evaluate antifouling strategies commonly employed throughout the literature against these requirements to determine those suitable for POC-based applications. These requirements are such that the biosensor must remain functional throughout the relevant detection time frame and any electrochemical background signals associated with nonspecific adsorption must be sufficiently low with respect to the required limits of detection for the target analyte.

This critical review highlights the main antifouling strategies used for electrochemical biosensors including nanoengineered surfaces (i.e., nanoporous metals and nanocarbons), antifouling layers (PEG, zwitterionic polymers, and biopolymers), nanoporous membranes, and hydrogels. Each antifouling strategy includes a discussion of the science behind the antifouling mechanism, the fabrication and synthetic techniques used, and the antifouling/electrochemical performance. In order to properly assess a given antifouling strategy for POC-based diagnostic relevance, we first introduce common and noteworthy practices in the field to highlight appropriate standard practices for evaluating antifouling strategies toward commercialization of electrochemical biosensors for POC applications.

One noteworthy practice commonly employed when evaluating antifouling strategies for electrochemical biosensing involves optimization of the incubation/rinse method. These experimental techniques typically involve an initial incubation step, where an antifouling-treated system is exposed to a fouling solution for a specific amount of time. The surface is then removed from the fouling media, rinsed with water or buffer solution, and then exposed to a solution containing the target analyte where electrochemical detection experiments are subsequently performed.[7−13] Incubation/rinse techniques of this type are not ideal for in situ analysis of antifouling performance as the rinse step may remove fouling molecules that are weakly bound to either the surface or the antifouling layer itself prior to conducting the electrochemical detection step. Even loosely interacting biomolecules can degrade signal fidelity and cause noise issues, particularly those that may impede the diffusion pathways of target analytes to the sensor surface. In a POC setting, it is generally not feasible to separate the analyte from the biological matrix. Consequently, electrochemical detection of the analyte must be accomplished within the biological matrix itself. Indeed, the incubation/rinse technique commonly employed throughout literature is not necessarily a good indicator of performance in real world POC settings. Incubation/rinse steps also create an opportunity for researchers to "massage" results by optimizing the incubation/rinsing parameters. This is commonly associated with experimental techniques where incubation times and conditions can be optimized or excessive rinsing can be used to reduce the amount of sensor fouling prior to the electrochemical detection step. In addition, fouling samples can become diluted and electrolyte conditions changed throughout the incubation, rinsing, and testing stages. Ideally, future investigation should strive to test sensor performance under the harshest conditions possible to properly evaluate the suitability of antifouling biosensor platforms for field-based POC applications.

The primary goal when evaluating the performance of electrochemical biosensors is to establish a correlation between the concentration of the target analyte and the resulting electrochemical signal. Obtaining this correlation involves conducting consecutive electrochemical measurements in a given fouling solution, where the target analyte concentration is varied between measurements. It is important to note that when conducting these experiments, it is recommended a fresh electrode surface is used for each new sample composition (i.e., change in analyte concentration) rather than simply rinsing or cleaning the sensor surface between experiments. Accumulation of both fouling molecules and/or target analyte can occur at the surface when the same electrochemical sensor is used repeatedly. In addition, the electrochemical signal can be compromised when unreacted analyte adsorbs directly to the electrode surface or indirectly through interactions with nonspecifically absorbed biomolecules. For field-based POC biosensing, a fresh biosensor should be used for each measurement and the resulting signal processed with a previously established correlation in order to accurately quantify the target analyte. Repeated exposure of a single sensor surface to fouling solutions containing analyte drastically compromises the ability to establish an accurate and reliable correlation between the signal and the changing analyte concentration. The standard practice for establishing a linear correlation between these should therefore treat each consecutive measurement as a "new test" similar to the procedure for a field-based POC test, where a fresh sensor surface would be used for each measurement. This practice prevents interference of residual fouling proteins/analytes present from previous measurements with the electrochemical signal and allows for an accurate conversion of the electrochemical signal into the analyte concentration.

When evaluating an antifouling strategy for a given biosensor platform, it is important to identify the target application and to use an appropriate sample matrix to assess fouling effects. The use of clean buffer solutions (i.e., PBS) at neutral pH levels,[14−20] single-molecule fouling solutions (i.e., bovine serum albumin (BSA) or fibrogen),[21−26] and even biological media which have been pretreated/diluted[27−32] are suitable for proof-of-concept experiments of antifouling capabilities; however they are not indicative of performance in complex biological media as highlighted by Ladd et al., in a study investigating the individual proteins in plasma responsible for surface fouling.[33] The study concluded that in single-protein fouling solutions antifouling performance is drastically

https://doi.org/10.1021/acssensors.1c00390
ACS Sens. 2021, 6, 1482−1507

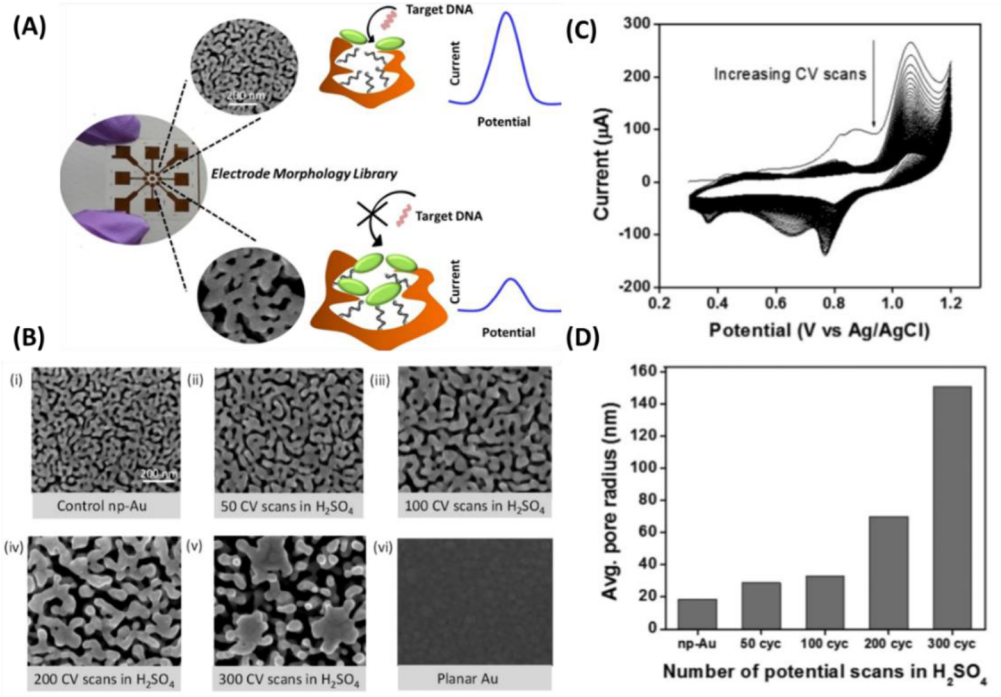

Figure 1. (A) Diagram of the multiple electrode array of nanoporous gold surfaces, (B) scanning electron microscope images of electrochemically coarsened surfaces with varying cycles in H_2SO_4 (i–vi), (C) cyclic voltammetry scans, and (D) average pore radius with respect to the number of coarsening cycles. Reprinted with permission from ref 41. Copyright 2017 American Chemical Society.

improved when compared with whole plasma. In addition, the pH of the sample has a significant impact on the charge density of many polymer-based antifouling layers, where more acidic/basic solutions can create the formation of defects within the antifouling layer and reduce the overall coating stability.[34] It is of importance here to suggest that a general framework should be developed for use in the field of antifouling coatings for electrochemical biosensors to reliably test/validate a platform. Understanding how a given antifouling strategy performs against the complex mixture of interfaces in complex biological solutions is paramount. If the primary objective is to develop an antifouling biosensor for commercial application, the sensor should be tested against the appropriate biological samples. Experimental evaluation should therefore include the detection of target analytes in the unprocessed biological samples.

■ NANOENGINEERED SURFACES

One of the most widely investigated strategies used to provide antifouling properties to electrode surfaces for biosensing applications is the use of nanoengineered surfaces. We generalize here that nanoengineered surfaces entail any surface with a nanomorphology or nanostructure. Nanoengineered surfaces can be comprised of a variety of different materials, namely, nanoporous/nanoparticle based metal surfaces (typically Au, Pt, and Ag)[16,35,36] and nanoporous carbon surfaces including carbon slurries, carbon nanotubes, or graphene and its derivatives (GO, rGO).[14,35,37,38] The large variety of electrode material and morphological combinations has generated a vast amount of research toward the fabrication and evaluation of different nanoengineered electrode surfaces for electrochemical biosensing. Nanoengineered electrode surfaces benefit mainly from ultrahigh surface areas which enhance the magnitude of the electrochemical signal.[39] Nanoporous electrodes harbor significantly more electroactive surface area than planar electrodes, and as a result the magnitude of the electrochemical signal, and hence sensitivity, has been shown to improve by at least an order of magnitude when compared with planar surfaces of like material.[40] The extremely high surface areas associated with these electrodes are the key to their good performance in highly fouling solutions. While the external surface of the nanostructure is exposed to the bulk solution and can become fouled (although to a lesser degree than planar electrodes), it is only a small portion of the overall electroactive surface area. Practically, the effect of fouling on the resulting electrochemistry is minimal as long as the analytes can reach the internal region of the nanostructure. This creates an intrinsic size-selectivity associated with nanoengineered surface morphologies via a "membrane-like" physical separation between the external and internal portions of the surface, where smaller molecules (i.e., analytes) can reach the interior surface and react with the electrode, while larger fouling molecules remain adhered to the external surface. This size-selectivity makes nanostructured surfaces good at facilitating electrochemical sensing of small molecules analytes even in highly fouling media.[41]

Investigation into the structure–property relationship between varying pore size/porosity and the resulting antifouling and electrochemical performances was investigated using a multiple electrode array comprised of nanoporous gold (npg) electrodes with different porosities to generate a "library" of morphologies.[41] Electrochemical coarsening was performed by exposing each npg electrode within the array to a different number of successive cycles in H_2SO_4, where longer cycling durations resulted in the formation of larger pores with lower overall porosities. The multiple electrode array included planar gold, a npg electrode without any coarsening, and four npg surfaces coarsened with 50, 100, 200, and 300 successive

https://doi.org/10.1021/acssensors.1c00390
ACS Sens. 2021, 6, 1482–1507

cyclic voltammetry (CV) cycles in 0.1 M H_2SO_4 as shown in Figure 1.

The degree of coarsening (i.e., etching of gold on the electrode surface) increased with increasing cycles in H_2SO_4 up to 200 cycles, where "islands" of gold began to form as the average pore radius increased, depicted in scanning electron microscope images taken of the different npg surfaces, Figure 1B. Electrochemical and antifouling characterization was then performed on the npg electrode array via electrochemical detection of surface bound thiolated probe DNA and complementary target DNA molecules in a buffer solution containing fetal bovine serum. The relationship between porosity and electrochemical signal and antifouling capabilities was highlighted by the size-selective characteristics associated with either smaller or larger pore diameters. Smaller pores exhibited the best performance for small molecule analyte detection via the size-selective filtering of large fouling molecules, while large pore diameters increased the accessibility of nucleic acids in the nanostructure at the expense of increased fouling exposure. The peak currents for the probe DNA molecules measured in solutions containing fetal bovine serum were found to decrease on surfaces exposed to high degrees of coarsening due to the reduced electroactive surface area; however, the signal for target DNA binding was increased via improved accessibility of the target DNA in the larger pores. The degree of coarsening and resulting pore size was therefore found to be inversely related with respect to each of these target analytes. The trade-off between available electroactive surface area and target DNA surface accessibility resulted in an optimal pore size of ∼30 nm for the detection of thiolated probe DNA and complementary target DNA molecules investigated here. The optimal pore size with regard to electrochemical and antifouling performance for nanoengineered surfaces therefore depends significantly on the sample composition (i.e., size of target analyte and potential fouling molecules in solution). The ideal nanostructured electrode morphology utilized for a given electrochemical biosensing application must be carefully considered with regard to both the total electroactive surface area (i.e., to achieve optimal peak current magnitudes), the pore to pore distance/uniformity, and the potential diffusional pathways that affect surface accessibility for both the target analyte and nonspecific adsorption of potential fouling molecules in solution.

NANOENGINEERED METAL-BASED SURFACES

Nanoporous metals are typically fabricated using a dealloying technique where one less noble metal is etched away from another within a metal composite. The most common example is the dealloying of Ag out of a bulk AuAg composite.[42] The bulk AuAg composite is immersed in nitric acid (HNO_3) for several hours to remove the Ag component leaving a nanoporous Au surface morphology. However, to prepare smaller metal nanoporous electrodes as opposed to bulk composites, microfabrication techniques such as sputter coating or lithography are typically used to coat the alloy onto a substrate resistant to the acid leaching dealloying process (i.e., SiO_2).[43] These microfabrication techniques are more suitable for developing npg electrodes for sensing applications, as they facilitate a traditional highly ordered 3D Au nanostructure, as opposed to the non-ordered nanoporosity that is typically created when using bulk dealloying processes. When using sputter coating techniques, for example, the ratio of sacrificial metal:gold within the alloy is a vital yet delicate parameter as it plays a significant role in the resulting porosity.[42] Once the substrate is coated with the alloy, it undergoes the same dealloying process using HNO_3 for several hours following the same mechanism as bulk composites. The resulting thin layer of nanoporous gold covering the substrate then needs to be integrated into an electrochemical sensing platform, which is typically achieved with use of laser etching to create the desired electrode shape or via standard lithography techniques to pattern the initial alloy before stripping.[41]

Nanoporous gold electrodes have been widely reported in the literature for use as antifouling electrochemical sensors.[8,21,22,35,40] The high electroactive surface area of the nanostructure allows for enhanced signal intensity while the porosity of the surface serves as a physical obstacle that prevents nonspecific adhesion of fouling proteins and macromolecules in solution. Many studies have demonstrated the excellent antifouling and detection capabilities of npg electrodes by conducting CV experiments in solutions containing commonly used fouling proteins such as fibrogen or BSA to compare the fouling effects and electrochemical performance between planar and nanoporous electrodes.[38,40,44,45] Although valuable, many investigations are often performed in solutions where the fouling molecules were present in relatively low concentrations (∼2 mg mL^{-1}) with only one or two different types of protein simultaneously. In addition, increasing the concentration of these single-protein solutions was shown to compromise the antifouling properties of the npg electrodes. CV experiments conducted in the presence of 16, 25, and 35 mg mL^{-1} BSA for 45 min of cycling exhibited decreases in peak current magnitude to 60%, 23%, and 4% of their original values when exposed to the increasing BSA concentrations, respectively.[21] Although these types of studies are crucial for evaluating the potential of npg-based electrodes for biosensor platform designs, they provide little information about how the system will perform in complex biological samples.[46] In solutions such as blood serum, urine, and saliva a range of fouling molecules are present both in high concentrations and with a variety of different molecular weights. The lack of data on the performance of npg-based biosensor platforms in untreated biological media is likely due to the detrimental effects of small molecule fouling via short peptides, proteins, or lipids present in these samples, an issue discussed by Ladd et al. in a study investigating the proteins responsible for surface fouling in plasma, highlighting the drastic differences between testing against diluted single-protein solutions compared with complex biological media.[33]

Modified nanoporous gold biosensing platforms were investigated for use in unprocessed biological media to assess the feasibility of npg biosensing assays for POC applications. The study conducted by Sabate del Rio et al. demonstrated an innovative approach to affinity-based biosensing using a three-dimensional matrix consisting of different nanomaterials (i.e., gold nanowires, nanoparticles, or carbon nanotubes) with an antibody functionalized composite coating for the detection of the inflammatory cytokine Interleukin-6 (IL-6) in unprocessed human plasma.[47] The developed composite coating comprised of glutaraldehyde, bovine serum albumin, and the bioreceptor for IL-6 was deposited onto a surface of planar gold. The approach aimed to pair the antifouling properties and functionalization capabilities of the bovine serum albumin/glutaraldehyde (BSA/GA) matrix with the good electron

https://doi.org/10.1021/acssensors.1c00390
ACS Sens. 2021, 6, 1482−1507

transfer that interlaced nanoengineered gold or carbon materials provides The developed BSA/AuNW/GA composite for the bioassay was as simple to produce as semipermeable membrane using off-the-shelf components. Using the sensor, a limit of detection (LoD) of 23 pg mL^{-1} was determined, showing good potential as a platform for sensing using bioreceptor−ligand binding. The sandwich immunoreaction occurs on the outside of the membrane, allowing only redox active species to diffuse through the semipermeable layer to the electrode surface.[48] The combination of a high electroactive surface area of a nanoengineered electrode with an antifouling strategy that does not significantly passivate the surface provides a promising and effective strategy toward electrochemical sensing in highly fouling biological media.

It is important to note, however, that for platforms which utilize separated and recessed electrode sites that are not directly in contact with the test solution, such as those existing within the pores of an antifouling matrix (i.e., dissimilar from typical nanoporous electrode surfaces), the electrochemical response can be impacted by the relationship between pore to pore distance and the resulting diffusion profile of the analytes. For a given nanoelectrode, the electrochemical signal profile is dependent on its the size, recess depth, pore to pore distance, time scale of the experiment, and the diffusion coefficient of the target analyte.[49] Assuming the nanoelectrode size and recess depths within each pore are relatively constant and the diffusion coefficient/experimental time scale are the same from experiment to experiment; the pore to pore distance most significantly affects the diffusion path of analytes and therefore the profile of the electrochemical signal. Figure 2 outlines different diffusion pathways taken by analytes in bulk solution for surfaces with both large and small pore to pore distances. The diffusion layers of the target analyte at each pore must overlap (i.e., the target analytes must arrive at the recessed electrode surface within the same relative time frame) to achieve a sharp peak current response, particularly at low analyte concentrations. When the pore to pore distance is large, Figure 2A, some analytes may take longer to reach the electrode surface (red arrows) which can result in undesirable peak broadening. When pore to pore distances are sufficiently small, Figure 2B, the resulting peak current response becomes sharper and larger in magnitude. This phenomenon has been previously observed in thermally swellable hydrogels where the swollen state results in larger pore to pore distances and broader electrochemical signal response profiles compared with the unswollen state.[50]

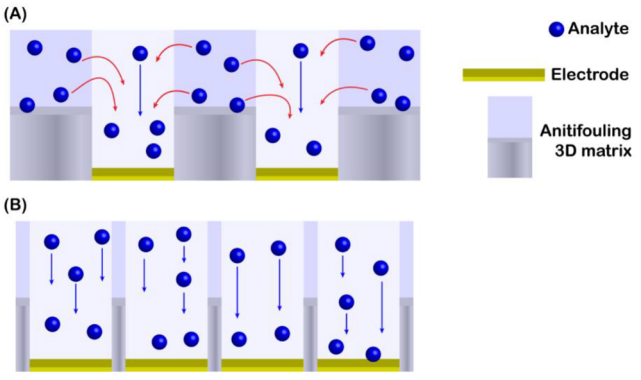

Figure 2. Schematic illustration highlighting the relationship between pore to pore distance and the resulting electrochemical response profile. The unshaded area in the fluid phase represents the area directly above pores within the antifouling 3D matrix, while the dark blue shaded area represents the area directly above the antifouling matrix. In systems with large pore to pore distances (A), some analytes can easily access the electrode surface within the pores (blue arrows) while others must take a longer diffusional pathway (red arrows). However, in systems with smaller pore to pore distances (B), a larger majority of analytes in bulk solution have rapid access to the electrode surface as a result of an increase in pore density. This can lead to more well-defined electrochemical signal responses, which is particularly advantageous for the detection of ultralow analyte concentrations.

As a result, it is important to create an antifouling matrix with sufficient porosity such that the recessed electrode sites are close enough to each other to allow overlapping diffusion profiles when conducting experiments such as square wave voltammetry (SWV) or differential pulse voltammetry (DPV) with constant scan rates. Overlapping diffusion profiles result in sharp/narrow peak current responses with larger magnitudes. In this regard, small pore to pore distances provide the capacity for obtaining a linear detection range at extremely low analyte concentrations and slow scan rates, where the peak current sensitivity toward the diffusion profile of analytes is typically more significant. The pore to pore distance in recessed electrode systems is therefore an essential parameter to consider in addition to the antifouling properties for a given biosensor design, as it is also directly impacted by the nanostructure, morphology, and composition of the electrode surface.

NANOENGINEERED CARBON-BASED SURFACES

Nanostructured carbon electrodes are another form of nanoengineering technology with applications in POC diagnostics and drug detection. Nanocarbon surfaces are typically synthesized by dispersing a form of carbon (i.e., nanotubes, nanoparticles, and nanosheets) in acid solution.[14,16,51] Nanocarbon electrodes are commonly fabricated using screen-printing and related techniques using slurries of carbon within a volatile liquid carrier and, in many cases, a polymeric binder or other functional additive for enhancing the electrochemical signal sensitivity or providing additional antifouling characteristics, some of which include ionic liquid composites,[52] or metal nanoparticles.[16] In addition, there are also a great deal of commercially available screen-printed carbon-based electrodes with surfaces containing various types of nanomorphologies and are arguably the most commercially successful nanostructured electrodes to date. This provides an intrinsic advantage for this technology when evaluating the suitability of nanocarbons for commercial biosensing applications. The ability to modify the nanostructured carbon surface once printed combined with the proven manufacturability makes these electrodes one of the most promising avenues toward commercially viable biosensor design.

Carbon-based electrode surfaces, namely, graphene and its derivatives, have been frequently utilized as electrochemical sensor surfaces throughout the literature. The widespread use of graphene and other carbonaceous materials for electrochemical sensing applications is likely a result of their exceptional electrochemical properties and ultrahigh surface areas, which facilitates extremely low limits of detection. In a review by Shao et al, the applications of graphene-based biosensors were highlighted including several platforms for the detection of dopamine,[53−55] glucose,[56,57] and DNA[58] in complex solutions.[59] One study involved a comparison

https://doi.org/10.1021/acssensors.1c00390
ACS Sens. 2021, 6, 1482−1507

between graphene oxide coated, graphite coated, and bare glassy carbon for the detection of several biomolecules, namely, the four free DNA bases and glucose for oxidase biosensing applications. Here the graphene electrode was able to simultaneously detect all four bases with specificity, whereas the graphite coated and bare glassy carbon electrodes could not.[58] In addition the nanoengineered graphene oxide electrode platform provided significantly lower detection limits for glucose when compared with other nanoengineered carbon surfaces including carbon nanotubes,[60,61] exfoliated graphite nanoplatelets,[62] carbon nanofibers,[63] and highly ordered mesoporous carbon.[64]

This result was attributed to the inherent fouling resistance of the nanostructured morphology of the graphene surface compared with the relatively planar glassy carbon morphology. The scanning electron microscope images in Figure 3A,B show

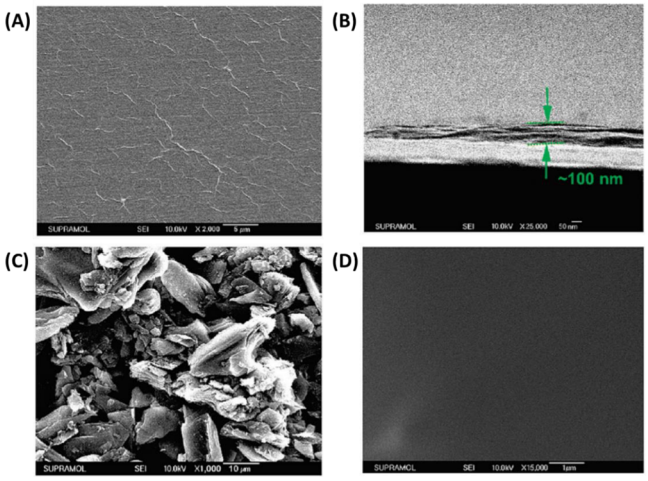

Figure 3. Scanning electron microscope images of the nanoengineered carbon surfaces including (A) graphene oxide, (B) side view image of the graphene oxide layer, (C) graphite, and (D) bare glassy carbon. Reprinted with permission from ref 58. Copyright 2009 American Chemical Society.

a layered and wrinkled paper-like structure for the graphene oxide coating, irregular shaped isolated graphite flakes, Figure 3C, and bare glassy carbon, Figure 3D. The wrinkles on the layered graphene oxide coating give rise to a high density of edge-plane defects, which drastically increase the amount of electroactive surface area compared to the other carbon-based surfaces, while the characteristically high conductivity of graphene increases electron transfer rates.[58] The combination of these properties enhanced the electrochemical signal magnitude and specificity of the system, allowing for improved electrochemical detection capabilities for glucose and DNA for the nanoengineered platform based on graphene oxide.

The ultrahigh surface area nanomorphology of graphene makes it an excellent electrode surface modification for electrochemical biosensing in complex sample matrices. Although fouling biomolecules can still adhere to graphene surfaces, there is a surplus of electroactive surface area available within the crevices, pores, and protruding edge-planes of the nanostructured graphene oxide surface to allow for sufficient electron transfer. Indeed, biomolecule fouling of graphene does not have a large impact upon the faradaic/charge transfer processes compared with lower surface area carbon surfaces (i.e., graphite, carbon nanofibers/nanotubes, carbon pastes, and glassy carbon). The capabilities of graphene and other nanostructured carbon surfaces to exhibit good electrochemical performance in complex media are not because of active antifouling mechanisms but rather its inherent decreased sensitivity to fouling. For the purpose of electrochemical performance and commercial application to POC diagnostics and biosensing, however, these mechanisms of fouling resistance serve the same purpose.

The literature investigating nanocarbon-based electrodes is extensive; however, their application in POC diagnostics and biosensing are not as widespread. Modified nanocarbon electrode surfaces have shown the ability to achieve extremely low LoD values in the nano-/picomolar range.[16,51] Although these electrodes possess excellent electrochemical signal sensitivity, the majority of results reported in the literature were achieved in buffer solutions (i.e., PBS) and provided little insight into how these systems perform in complex biological media. From a manufacturing perspective, composite nanocarbon systems including additives such as ionic liquids, coatings of mixed dispersions, or metal nanoparticles often involve long fabrication processes (i.e., 24 h refluxing, overnight drying, or material synthesis).[14,15,27] These additional treatment steps significantly complicate manufacturing when compared with bare screen-printed nanocarbon electrodes. To translate nanocarbon-based electrode sensing platforms into commercial products, research should be aimed at the detection of clinically relevant target analytes in complex biological media, while simultaneously enhancing the simplicity of manufacture of the sensing platform.

Electrochemical detection of Modafinil in unprocessed saliva samples was performed on carbon nanotube (CNT) based

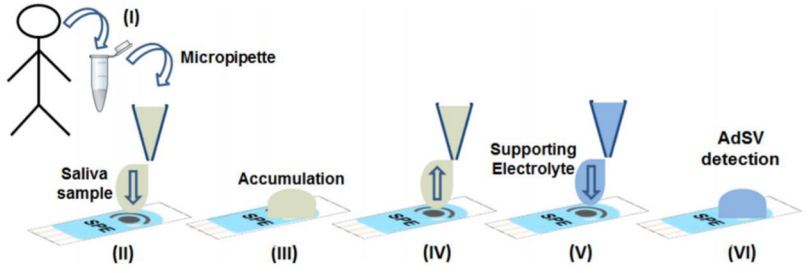

Figure 4. Schematic illustration showing the experimental procedure for the preconcentration and POC-based detection steps of Modafinil in saliva samples. Steps I and II show the initial deposition of the saliva sample onto the electrode surface containing Modafinil; III shows the accumulation step where a potential is applied to draw Modafinil to the electrode surface IV and V illustrate that the sample is then removed and supporting electrolyte is added; and finally VI shows the electrochemical detection is performed on the Modafinil accumulated at the electrode surface in a supporting electrolyte solution. Reprinted with permission from ref 9. Copyright 2019 Elsevier.

https://doi.org/10.1021/acssensors.1c00390
ACS Sens. 2021, 6, 1482−1507

Table 1. Different Analytical Methods Reported for the Detection of Rohypnol Including the Analytical Linear Range of Detection and the Limit of Detection (LoD) in Various Complex and Clinically Relevant Media (Reprinted with Permission from Reference 65. Copyright 2013Royal Society of Chemistry)

analytical method	analytical linear range	LoD	matrix	comments
gas chromatography−mass spectrometry	Δ	0.1 pg mL^{-1}	oral saliva	only detection within 12−24 h of sample collection
liquid chromatography−atmospheric pressure chemical ionization mass spectroscopy	1−500 $\mu g\ L^{-1}$	0.2 ng mL^{-1}	human serum	extensive sample preparation
HPLC-UV vis	Δ	1 ng mL^{-1}	human serum	excellent recovery from serum samples
fluorescence spectroscopy	0−5 mg L^{-1}	1 ng mL^{-1}	beverage	only clear samples analyzed, time-consuming process
HPLC-multiwave	0.01−5 mg L^{-1}	5 ng mL^{-1}	human serum	quantification limit of 10 $\mu g\ L^{-1}$
HPLC-dual electrode detection	0−1 mg L^{-1}	20 ng mL^{-1}	beverage	dual electrode system consisting of a carbon fiber veil and glassy carbon electrodes
this work	1−95.24 $\mu g\ L^{-1}$	0.47 $\mu g\ L^{-1}$	buffer, beverage	proof-of-concept in colored beverages; no sample preparation needed
desorption electrospray ionization−mass sectroscopy	3−20 $\mu g\ L^{-1}$	3 $\mu g\ L^{-1}$	beverage	no sample preparation needed
gas chromatography−electron capture	25−300 ng L^{-1}	1 mg mL^{-1}	human serum	lengthy analysis time up to 1 h

screen-printed electrodes, with a linear detection range of 50−500 μM with an LoD of 2 μM without interference from ascorbic or uric acid. However, a preconcentration step was used for the detection experiments, as shown in Figure 4.

The detection process here involves an initial sample acquisition onto the sensor (I, II) followed by an applied potential in order to accumulate the drug (III), where the saliva is subsequently removed from the sensor and supporting electrolyte is added (IV, V) prior to the electrochemical detection (VI). Although the preconcentration step ensures all Modifinil within the sample is detected, the removal of the saliva sample and subsequent addition of supporting electrolyte could potentially alter the concentration of analyte measured (i.e., concentration detected lower than original concentration). Experimental steps which involve the addition, subtraction, or transfer of fluid introduce a source of sampling error associated with the ability to accurately measure liquid volume and unwanted liquid retention in the transfer vessel (i.e., fluid films on the pipet walls, trapped meniscus in the pipet, and adsorption of analyte to solid surfaces during transfer), as well as the potential for sample contamination, user error, and erroneous results. It also is not conducive to a POC setting as likely trained personnel or complex automation is required for proper liquid handling and event timing.

Detection strategies involving meticulous preconcentration or pretreatment steps are not feasible for rapid POC diagnostics/detection applications such as those required by paramedics, doctors, or police officers, however can be appropriate for in-house detection applications such as drug tests for athletes or workers where additional steps can be easily performed in time-independent and environmentally stable situations. Experimental methodologies involving sample pretreatment or analyte extraction steps are effective strategies for applications with readily accessible laboratories and are best compared with established competing technologies such as high-performance liquid chromatography (HPLC).

POC-based electrochemical detection with no sample treatment or analyte concentration steps was demonstrated on graphite screen-printed electrodes for the detection of Flurnitrazepam (Rohypnol), a benzodiazepine drug compound commonly discovered in beverages associated with criminal date rape cases.[65] Detection experiments were performed in the raw untreated international beverages Coca-Cola and alcopop WKD with aim toward forensic analysis of crimes involving spiked alcoholic beverages. Linear detection capabilities (1−245.6 $\mu g\ mL^{-1}$) were achieved in both beverages with a LoD of 0.47 $\mu g\ mL^{-1}$, demonstrating a proof-of-concept in situ electrochemical detection. The strategy used provided rapid results in raw untreated samples and highlighted a good practice within the field of POC-based electrochemical biosensing.

Although the LoD for this system was higher than many laboratory-based strategies, Table 1, the graphite screen-printed electrodes used were not supplemented by any type of antifouling modification. Electrode surface fouling is likely a primary cause for the high LoDs achieved by the bare graphite screen-printed electrodes. The approach involving screen-printed nanocarbon electrodes provides an already commercially manufactured option compared with nanoengineered metals which involve a more expensive and complex fabrication process. Combining the intrinsically high electroactive surface areas of screen-printed nanocarbons with commercially viable antifouling coatings/composites is a promising avenue to pursue and should help push the limits of detection achieved by bare nanocarbon surfaces to even lower values.

ANTIFOULING COATINGS

Many recent approaches toward the development of electrochemical biosensing platforms are primarily focused on the integration of antifouling coatings with the sensor surface. One of the major advantages for the use of antifouling coatings on electrode surfaces is the wide range of different polymers and end-group functionalizations that can be employed in order to tailor the antifouling mechanisms. Although the many types of antifouling coatings throughout literature are well-documented, only some are suitable for use in electrochemical biosensing applications. One significant issue with antifouling coatings is electrode passivation, where coatings grafted to an electrode surface occupy a portion of the surface area thus reducing the amount of surface capable of participating in electrochemical reactions or charge transfer processes. This effectively creates the same issues for biosensors as surface fouling does, where the overall electrochemical signal magnitude is reduced as a result of diminished electrode surface accessibility for the target analytes. The primary challenge is thus devising antiadhesive coatings systems which

https://doi.org/10.1021/acssensors.1c00390
ACS Sens. 2021, 6, 1482−1507

can effectively prevent fouling without concomitantly passivating the electroactive surfaces.

Surface coatings based on self-assembled monolayers (SAMs) of poly(ethylene glycol) (PEG) and its derivatives oligio(ethylene glycols) have been widely used in biomedical applications as PEG chains can be easily tethered to a wide range of surfaces and are both a nontoxic and nonimmunogenic polymer.[66−70] Research within the field of antifouling surface coatings has also been expanded over recent years toward alternatives to PEG and its derivatives, namely, different zwitterionic polymers,[71,72] poly(2-oxazolines),[73−76] and various biopolymers including short-chain amino acids (peptides) and glycoproteins such as lubricin (LUB).[1,77−80] The antifouling efficacy of polymer-/biopolymer-based antifouling coatings can be altered via different grafting approaches. The coatings can be "grafted-to" the electrode surface through covalent binding to create a linear polymer brush,[81] or can be "grafted-from" the surface via surface-initiated atom transfer radical polymerization (SI-ATRP) or electropolymerization.[82−86] Typically, polymer-/biopolymer-based coatings are integrated onto the surface as linear brushes of self-assembled monolayers (SAMs), which have been shown to significantly prevent bacterial adhesion in biomedical implants.[87] The antifouling capabilities for grafted-to SAM coatings are determined primarily by the degree of molecular hydration or how strongly bound water molecules are around the chains of the SAM layer. As outlined by Whitesides et al., inert surfaces typically exhibit polarity, possess hydrogen-bond acceptors, have no hydrogen-bond donors, and are electrically neutral; all of which support the hypothesis that strong interactions between functional groups of SAMs and water are a common phenomenon associated with antifouling characteristics for a surface.[88] Secondary factors which affect the antifouling properties of SAM coatings include polymer grafting density, chain length, conformation, and end-group chemistry, which all play interrelated roles and alter the antifouling mechanism in different ways, making it difficult to isolate the degree of influence for each property when evaluating a specific coating.[89]

The hydrophilicity of most polymer/biopolymer coatings is the primary antifouling mechanism which operates via a reduction in the nonpolar interactions between fouling molecules and the individual polymer chains of SAM brushes.[77] These binding interactions within the brush produce a highly hydrated environment within the antifouling coating, which target analytes can diffuse through while simultaneously creating a steric repulsive barrier that fouling molecules must supplant before adhesive bonds can be formed with coating molecules. While the grafting density is directly proportional to the amount of physical blocking between fouling molecules and the electrode surface via steric hindrance, brush density also directly impacts the entropy barrier created by excluded volume effects.[89] The combination of large steric forces and the increased entropy barrier associated with high coating densities repels proteins from entering the coating and binding to the electrode surface. Consequently, "soft" adhered proteins and macromolecules may accumulate directly above/within the polymer brush, a phenomenon often observed in the results of rinsing steps which remove loosely bound proteins from antifouling layers.[7,90] Large aggregations of these weakly associated fouling molecules can affect the diffusion path target analytes must take when moving from bulk solution to the electrode surface. The hindered diffusion profile of target analytes within this environment can become detrimental to the electrochemical signal magnitude, making it difficult to quantify extremely low analyte concentrations in highly fouling media. Therefore it is imperative to consider how the various antifouling mechanisms of a coating operate, as properties that are beneficial in isolation may behave synergistically toward the detriment of the desired target application.

Although PEG/OEG are considered the "gold standard" of antifouling coatings, much research into zwitterionic polymers/biopolymers alternatives has gained traction over the past 10−15 years due to the stronger hydration effects associated with the differently charged groups attached to the neutral polymer backbone leading to enhanced antifouling properties.[77] Zwitterionic polymers have the additional capability to create switchable surfaces between cationic, anionic, and zwitterionic states and can be easily integrated with various nanoparticle-based systems.[29,91] Some of the common zwitterionic species investigated include a range of polymethacrylates and amino acids (i.e., peptides based on the EK sequence).[92−94] Zwitterionic-based coatings utilize similar antifouling mechanisms to traditional SAM coatings primarily via the degree of hydration, but the chain density, length, and conformation also play significant roles while the end-group charges and functionality serve as additional components to consider.

Many of these properties are related to the fabrication method used to apply the antifouling coating to a given surface, where different grafting methods can provide functional tailorability in the resulting layer. While traditional antifouling polymer coatings (PEG/OEG) are grafted-to via covalent bonding to the surface to create SAMs, methacrylate-based zwitterionic coatings such as oligo(ethylene glycol) methacrylate, sulfobetaine methacrylate, and carboxybetaine methacrylate were grafted-from the surface via SI-ATRP in a study comparing the different polymer coatings.[33] SI-ATRP involves the use of a transition metal catalyst with an alkyl halide (R−X) initiator, where the catalyst determines the polymerization rate and the amount of initiator determines the number of polymer chains grown. During the growth process each polymer chain has the same probability to propagate resulting in the formation of polymers with similar molecular weights and molecular weight distributions.[95] The ATRP processes therefore allow for a high degree of tailorability in terms of the resulting polymer chain length and density via changes in the initiators/catalysts used compared to traditional grafted-to SAMs of OEG. This facilitates the ability to use platforms based on grafted-from zwitterionic coatings for a wider range of applications as the chain density and length can be altered.

One unique and innovative strategy to combat biofouling for electrochemical sensors was conducted by Wang et al, where transient methacrylate based polymer coatings were used for delayed exposure of fresh electrode surfaces.[96] The approach involves turning "on" the different sensor surfaces of the multielectrode array at preselected sequential times. In this way the sensor surface is kept pristine until the moment that the electrochemical measurement is performed, therefore limiting the amount of time in which biofilm formation could occur. The time frame of the electrode exposure can be optimized for samples with specific pH levels via altering the dissolution rate of the methacrylate polymer layer, which is directly dependent on the thickness and density of the coating. This concept provides the ability to conduct long-term electrochemical

https://doi.org/10.1021/acssensors.1c00390
ACS Sens. 2021, 6, 1482−1507

monitoring in highly fouling biological environments as each electrode surface can perform the same measurement as they are sequentially exposed to the solution, as depicted in Figure 5.

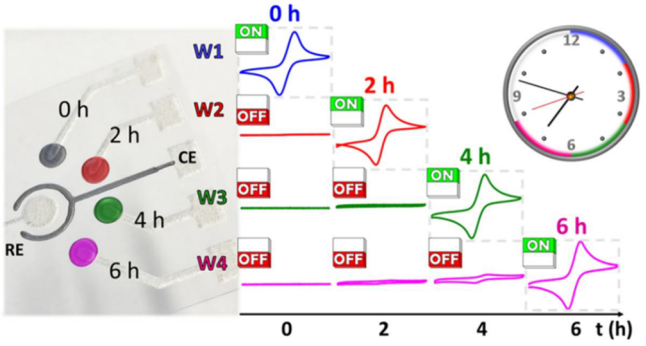

Figure 5. Illustration of the multielectrode array coated with methacrylate polymer layers of four different densities and thicknesses and the corresponding cyclic voltammograms associated with them. Each layer is tailored to dissolve within 2 h of the previous layer, which allows for identical cyclic voltammetry responses 6 h apart. Reprinted with permission from ref 96. Copyright 2018 American Chemical Society.

The potential for commercial application of pH responsive delayed sensor activation platforms in the field of biosensors is promising, particularly for electrochemical diagnostics in acidic environments such as gastrointestinal fluids or urine. Edible biosensors based on this platform were fabricated using carbon paste electrodes prepared using edible materials such as olive oil or charcoal.[97] These studies highlight an innovative use of widely available methacrylate-based polymers and cost-effective electrode platforms for a specific range of commercial applications.

Biopolymers serve as another alternative antifouling polymer coating candidate which can overcome some limitations posed by traditional polymer coatings, mainly biodegradation. Potential biopolymer candidates include a variety of small chain amino acid peptides, various carbohydrates, and the glycoprotein LUB present in the articular joints of mammals, which can all be implemented as SAM-based antifouling coatings onto various substrates.[98−101] The peptide sequence containing alternating lysine (K) and glutamic acid (E) groups is widely popular because EK sequenced peptides are the most abundant amino acids present in the interior of molecular chaperones, which are the proteins associated with the conformational folding and unfolding or assembly/deassembly of macromolecules.[1,102−106] EK sequenced peptides also interact more strongly with water molecules than other peptide chains. As previously discussed, strong interactions between functional groups and water molecules result in better antifouling properties making EK-based peptides a logical choice for investigation as an antifouling candidate. Certain carbohydrates likewise result in strongly bound hydration shells due to the geometry of the saccharide units which promotes efficient packing of water molecules around them. These strongly hydrated saccharides include galactose, sialic acid (i.e., a functional group populating the molecular backbone of LUB molecules), chondroitin sulfate, and *N*-acetyl-D-glucosamine and have been used as antibacterial and antifouling coatings for biomedical applications.[107−109] Antifouling coatings based on these biomolecules have the advantage of being inherently biocompatible and commercially available. The behavior of these molecules with respect to proteins in the biological environment where they typically exist can provide valuable insight into how they might behave when exposed to different fouling solution compositions.

POLY(ETHYLENE GLYCOL)

There are several effective ways to synthesize poly(ethylene glycol) (PEG) antifouling brush coatings, all of which directly impact the different characteristics and performance of the coating. Linear polymer coatings of end-functionalized PEG can be easily applied to a surface as SAMs using the grafting-to approach via chemisorption. Utilization of high-density polymers with consistent molecular weight distributions facilitates a 3D structure where the "head groups" of the polymer chain bind with the surface allowing for the "tail-end groups" to extend into the solution creating a molecular brush.[81] The most common PEG-based SAMs include oligoethylene glycol terminated alkane thiols, although a wide variety of different tail-end functional groups and ethylene glycol (EG) backbones can be implemented, including hydrophobic methyl terminated and hydrophilic hydroxyl terminated end groups.[110] The self-assembly mechanism allows for simple surface application while the vast range of functional group modifications provides functionality customization. However, strong surface interactions for SAM-based coatings are restricted to metal-based surfaces and the nature of monolayered coatings yields a limited robustness, often leading to defects in the resulting PEG layer.[111,112] Non-uniformity via these defects can have a profound effect on the overall antifouling capabilities of surface coatings, particularly for applications in electrochemical sensing where surface defects can leave portions of the sensor surface exposed to the fouling media. To overcome the limitations associated with SAMs of PEG, other grafting strategies have been explored.

Another adopted strategy for the formation of PEG-based antifouling coatings involves an in situ process of PEGylated (i.e,. polymer chains containing PEG side groups) coatings using surface-initiated polymerization, by which a linear brush of polymers is grown at the surface via the grafting-from approach.[113] The general SI-P process involves the immobilization of a specific initiator from which a target monomer is solely grown from. There are many different SI-P-based techniques, primarily SI-ATRP because it is compatible with a range of initiator and monomer functional groups and provides good control over the polymerization kinetics providing tailorability in the polymer brush characteristics.[114] The SI-ATRP process is outlined in Figure 6 where an oligoethylene glycol methacrylate based polymer coating was grown on gold and glass substrates.[69,115]

The SI-ATRP-based grafting-from approach has been shown to overcome many of the limitations associated with SAM-based PEG coatings. ATRP initiators can be easily immobilized on surfaces through chemical self-assembly or covalent binding. The "footprint" (i.e., amount of surface area occupied) of the initiators is drastically less than the oligoethylene glycol methacrylate polymer grown from it, therefore maintaining a larger electroactive surface area for electrochemical detection applications. The active polymerization allows for control over the density and thickness of the polymer brush, which provides a significant degree of control over the resulting antifouling characteristics.[69] Despite the

https://doi.org/10.1021/acssensors.1c00390
ACS Sens. 2021, 6, 1482−1507

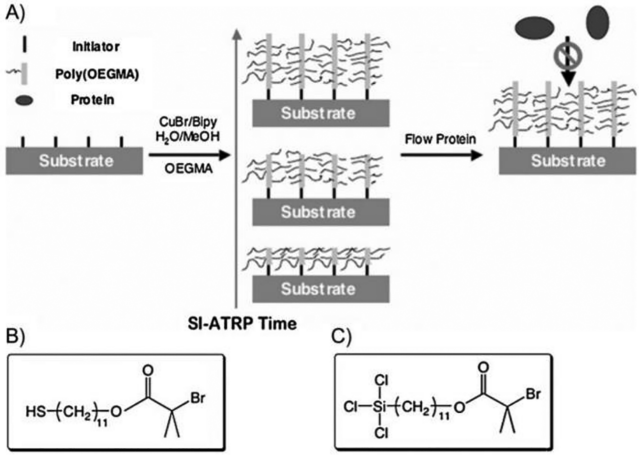

Figure 6. Schematic illustration showing the SI-ATRP growth process for surface-initiated polymerization of SAM PEG coatings. (A) Attachment of poly(OEGMA) strands to the surface initiators over time to create a protein resistant surface, and the molecular structures of (B) thiol-terminated initiator and (C) silane-terminated initiator. Reproduced with permissions from ref 69. Copyright 2009 WILEY-VCH Verlag GmbH & Co. KGaA, Weinheim.

numerous benefits exhibited by grafting-from approaches for the formation of PEG-based antifouling coatings, the requirement for initiators and the polymerization process make commercial manufacturability an issue to consider. Mass production of single-use POC biosensors requires large scale application of antifouling coatings to individual electrode surfaces, where a simple one-step coating application process is more commercially feasible.

The literature on PEG and its derivatives as candidates for antifouling coatings is extensive as they have been shown to be widely successful for a range of applications from large implants to smaller surface area biosensors.[77] However, the majority of research investigating the antifouling capabilities of PEG has been focused on single-molecule solutions containing proteins notorious for their fouling characteristics, namely, fibrogen (FB), BSA, and immunoglobulin G (IgG). Various electrochemical experiments on electrodes modified with PEG including PEGylated Pt[7] and GC modified with PANi/PEG nanofibers[10] showed a resistance to fouling in these single-protein solutions. The fouling resistance is primarily associated with interactions between bound water molecules within the coating, which give rise to a degree of hydration forces which depend on the hydrophilicity of the PEG chains and water packing efficiency. It has been shown that PEG coatings with long-chain monomers and high packing density at the surface can improve biofouling resistance; however, increasing these parameters can have a detrimental effect on the electrochemical performance as the anchoring groups of the PEG coating significantly passivate the electrode surface and long-chain monomers create a more tortuous diffusional pathway for analytes traveling from bulk solution to the electrode surface. The inverse relationship between antifouling capabilities and electrochemical performance with respect to PEG coating density/chain length has been documented using impedance and quartz crystal microbalance analysis[116] and on ionic screening of analyte charges for transistor-based biosensing.[116,117]

A promising strategy toward overcoming the decrease in signal sensitivity associated with PEG coatings is through combining high surface area electrodes and/or nanoparticles with the PEG antifouling coatings to maintain a high electroactive surface area while simultaneously preventing nonspecific adsorption of fouling proteins.[19,23] While the studies implementing these composite systems show linear analyte detection ranges and low LoDs, the detection experiments are typically performed in clean buffer solutions. Although further investigation for these types of biosensing platforms in complex biological media is required, the approach of combining antifouling coatings with high surface area nanostructured electrodes have the potential for exploiting the advantages and negating the drawbacks that would be associated with each strategy in insolation.

Many electrochemical detection strategies for PEG coated biosensors involve an incubation of the electrode in the fouling solution followed by rinsing prior to performing the electrochemical measurement. This problem was highlighted in a study identifying the proteins responsible for fouling surfaces modified with PEG-based coatings.[89] Resistance to fouling via the main proteins in blood (i.e., albumin, IgG, and FB) was achieved in single-protein solutions of each; however, residual surface fouling was consistently observed in complex biological solutions such as human blood plasma. As a result, the antifouling performance of PEG coatings in single-protein solutions typically appears strong, while in complex solutions, where smaller proteins can also adsorb to the surface, they are much less effective. The study by Riedel et al.,[89] found that large proteins such as albumin, IgG, and FB weakly interact with both the PEG coatings themselves and with smaller fouling proteins in the blood plasma. The removal of large proteins from plasma (i.e., large lipid transporting apolipoproteins and FB) through a 300 kDa filtration step led to the absence of these proteins on the tested deposits; however, additional smaller proteins were also absent from the deposits after filtration, indicating that the surface adsorption of some smaller proteins was mediated by the larger ones. Therefore when a system is rinsed prior to measuring the degree of fouling, these proteins are washed away creating a "false" determination of antifouling performance when the subsequent electrochemical detection measurements are performed.

The weak binding interaction exhibited between small proteins and larger proteins in solution is a characteristic that is likely shared by target analyte species in solution. There are many examples where cationic (and anionic) small molecules or even target analyte drug compounds complex with the various proteins in biological media. The binding interaction between one such target analyte clonazepam (i.e., benzodiazepine-based drug compound) and large fouling proteins in saliva has been analyzed, particularly with respect to the effect of these interactions on the electrochemical detection of analytes in fouling solutions.[118] Interestingly, peak current responses were obtained for clonazepam on severely fouled reduced graphene oxide electrodes tested in unprocessed saliva samples, and even as the concentration of Cz was changed in subsequent experiments, the current magnitude remained constant. Cz is known to exhibit a strong binding affinity (≥88% bound) toward proteins in serum among other epileptic drugs.[119] It was hypothesized that the available binding sites on the fouling proteins present in saliva became saturated with Cz molecules. Once these proteins nonspecifically adsorbed to the bare electrode surface forming a biofilm, free Cz molecules in solution could no longer reach the electrode surface. As a result, the electrochemical signal

https://doi.org/10.1021/acssensors.1c00390
ACS Sens. 2021, 6, 1482−1507

Table 2. Charge Transfer Resistance of Different Mixed Zwitterionic Coatings on Glassy Carbon and Gold for the Differently Charged Species $Fe(CN_6)^{3-}$ and $Ru(NH_3)^{3+}$ before 1 h of BSA Adsorption and after 1 h of BSA Adsorption (Reprinted with Permission from Reference 24. Copyright 2013 American Chemical Society)

	R_{ct} (Ω cm^2) (in $Fe(CN_6)^{3-}$ solution)		R_{ct} (Ω cm^2) (in $Ru(NH_3)^{3+}$ solution)	
	before 1 h BSA	after 1 h BSA	before 1 h BSA	after 1 h BSA
PPC-GC	809.3(s = 15.7)	807.9(s = 16.7)	42.3(s = 1.1)	44.3(s = 1.1)
mix-GC	185.6(s = 2.0)	178.3(s = 1.9)	26.02(s = 1.24)	25.2(s = 1.3)
OEG-Ph-GC	1899.3(s = 2.0)	3734.1(s = 233.3)	192.6(s = 3.1)	556.4(s = 9.6)
OEG-SAM-Au	10342.2(s = 130.9)	10226.5(s = 131.1)	6299.4(s = 296.7)	6222.3(s = 315.7)
C12-SAM-Au	30874.6(s = 1423.4)	49461.7(s = 1821.4)	14373.2(s = 157.6)	18947.9(s = 183.4)
bare GC	15.3(s = 0.7)	92.3(s = 1.1)	1.3(s = 0.9)	19.2(s = 1.3)
bare Au	10.3(s = 0.6	29.2(s = 0.6)	0.8(s = 0.2)	11.5(s = 1.5)

magnitude obtained was directly associated to the amount of bound Cz within the biofilm as opposed to the total concentration in solution. This effect was supported by the constant electrochemical signal obtained on the fouled rGO surfaces with respect to changes in the Cz concentration in solution, where concentrations ranging from 25 nM to 2.5 μM had no effect on the electrochemical signal of the system. This phenomenon further supports the severity of the issue with electrode rinsing steps in electrochemical detection experiments, where rinsing away the biofilm accumulated at an electrode surface can also remove target analytes and smaller fouling species from the solution. Rinsing away these components can result in the inability to accurately correlate analyte concentration added to the solution with the electrochemical signal magnitude measured and may additionally remove fouling components from the sample.

Despite the fact that PEG-based coatings are among the most widely used antiadhesives, they have yet to find broad commercial success in electrochemical technologies. Further investigations of PEG-based coatings should be focused on in situ electrochemistry of unprocessed biological media (i.e., blood plasma, serum, saliva, or urine) rather than using incubation/rinse steps or single-protein fouling solutions in order to realize applicability toward POC-based biosensing applications.

THIOLATED POLYMERS AND ZWITTERIONIC COATINGS

Much of the investigation into alternatives to PEG and its derivatives for application as antifouling layers has been focused around different thiolated self-assembled monolayer and zwitterionic-based polymer coatings. Zwitterionic coatings have been primarily comprised of long-chain alkane thiol based SAMs modified with zwitterionic moieties.[120,121] These zwitterionic coatings however still suffered from issues similar to those of PEG-based coatings, namely, high electrochemical impedance as a result of the high grafting density of the SAM and the large coating thickness associated with the long-chain conformation.[24] In order to create a less tortuous diffusion path for analytes traveling between bulk solution and the electrode surface, alkane thiol based SAMs with a high density of short ethylene glycol oligomers were investigated and showed antifouling characteristics similar to those of traditional PEG layers.[120] However, it was shown that short-chain alkane thiol based SAMs suffered from poor conformational stability compared with long-chain alkane thiol SAMs.[122] While it is possible to incorporate various zwitterionic moieties into both long- and short-chain alkane thiol SAMs to improve the antifouling characteristics via stronger hydration effects associated with the charged terminal groups,[77,123,124] further investigation into these coatings was aimed at reducing the electrochemical impedance and stability issues associated with the chain length/structure of the alkane thiol based SAM backbones.

Traditional two-component alkanethiol derived SAMs based on 6-mercaptohexanol (MCH) and thiol-derivatized single-stranded oligonucleotide probe (thiolated capture probe, SHCP) are commonly used for antifouling studies as an alternative to PEG-based coatings.[125−127] However, these two-component SAMs have been shown to suffer from nonspecific background signals and related surface defects leading to low reproducibility.[128] In order to combat this issue Wu et al., implemented a ternary monolayer through the addition of α,ω-alkanedithiol dithiothreitol to the SAM for the ultralow detection (Zepto-molar) of nucleic acid hybridization without any signal amplification in complex samples of urine and serum.[129] This extremely low detection limit was attributed to both a reduction in "pinhole" defects within the monolayer as a result of a more uniform and dense surface coverage and the OH-richer hydrophilic environment at the surface leading to a significant resistance to nonspecific adsorption.

Another strategy conducted by Jolly et al., investigated to address the electrochemical impedance and stability issues associated with some of the traditional betaine-based SAMs.[130] These authors developed an aptamer-based biosensor for the detection of prostate specific antigen in real blood samples using a new class of thiol-terminated sulfo-betaine SAMs as spacer molecules. Electrochemical impedance spectroscopy was used for clinical application of the aptamer-based biosensor where a SAM of MCH and thiolated-DNA aptamer were compared to the thiolated sulfo-betaine and amine-terminated aptamer layer. It was found that the thiolated sulfo-betaine spacer molecules within the layer of the latter prevented nonspecific binding of the control protein human serum albumin and reduced the charge transfer resistance of the system when compared to the traditional MCH-based SAM (further highlighting the nonspecific binding issues of MCH-based SAMs as highlighted above), allowing for the label-free detection of PSA levels lower than 1 ng mL^{-1}. This new class of SAM exhibited equal or better performance compared with PEG and traditional betaine-based SAMs primarily due to the improved stability of the monolayer that the small chain length sulfobetaine spacers within the system provided which improved resistance to nonspecific binding and reduced the overall charge transfer resistance of the coating.

Further investigation looked into novel organic SAM coatings that were synthesized using simple aryl diazonium salts with the purpose of creating an antifouling zwitterionic

https://doi.org/10.1021/acssensors.1c00390
ACS Sens. 2021, 6, 1482−1507

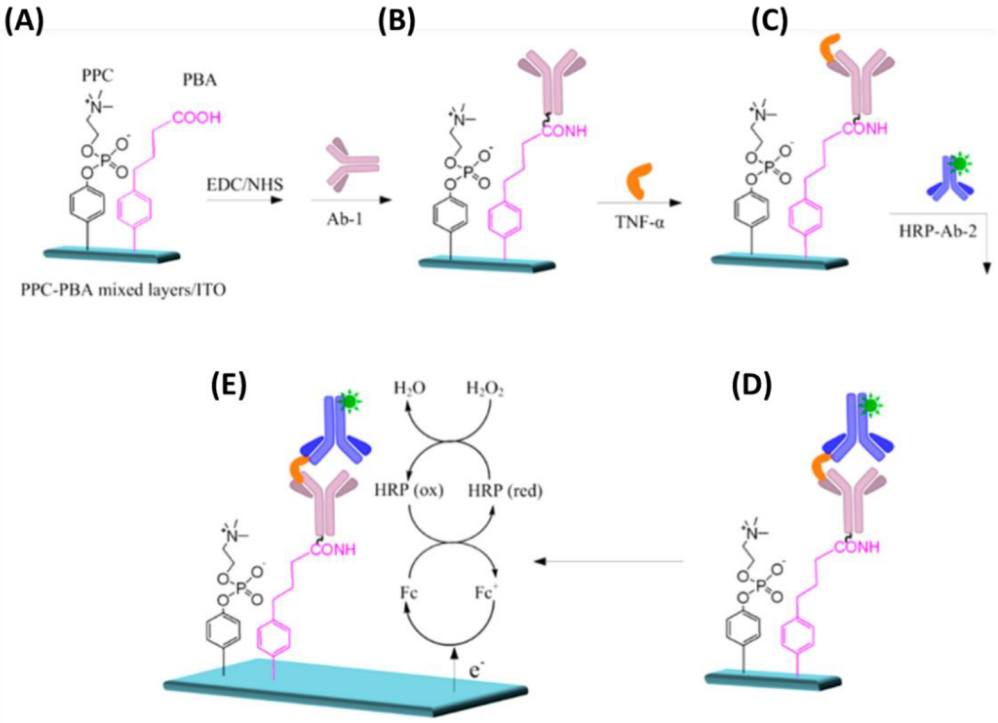

Figure 7. Schematic illustration of the "sandwich assay" format of detection for a mixed Zw coating of PPC−PBA. (A) Initial deposit of the coating on ITO substrate, (B) immobilization of Ab-1 antibody, (C) TNF-α binding to the Ab-1 antibody (biorecognition element), (D) HRP-Ab-2 attachment, and (E) enzyme-dependent HRP reaction of H_2O_2 with ferrocenemethanol creating an electron shuttle with the surface. Reprinted with permission from ref 11. Copyright 2016 American Chemical Society.

coating which simultaneously possessed low electrochemical impedance, electrode passivation, and conformational stability of the SAM.[131] Zwitterionic SAMs based on phenyl anchoring groups derived from aryl diazonium salts have been shown to prevent BSA adsorption more effectively and with lower charge transfer resistances and electron transfer kinetics compared with zwitterionic alkane thiol based SAMs in incubated solutions of BSA.[24] The results shown in Table 2 highlight the utility in combining zwitterionic functional groups with aryl diazonium salt derived phenyl anchoring groups to create low impedance and surface coverage antifouling SAM coatings compared with traditional long-chain zwitterionic alkane thiol based SAMs.

The use of zwitterionic antifouling coatings for applications in electrochemical biosensing has therefore shifted toward incorporating different phenyl anchored zwitterionic species within the same SAM coating. The advantages of mixed zwitterionic phenyl layers was realized in a study combining phenyl phosphorylcholine (PPC) and phenyl butyric acid (PBA), where the PPC chains served as the antifouling component of the layer (PPC "mimics" the head group of many common lipids which have intrinsic low adhesion properties) and the PBA allowed for bioconjugation with specific antibodies (biorecognition element) for electrochemical detection purposes.[11] The sensing principle for this system was based on an enzyme-dependent reaction associated with the HRP mechanism (based on H_2O_2) and the redox mediator ferrocenemethanol to facilitate an electron shuttle for the detection of tumor necrosis factor α (TNF-α), Figure 7.

The immunosensor presented implements a so-called "sandwich assay" format of detection requiring a series of incubation steps. The PPC−PBA aryldiazonium mixture is first generated in a solution of HCl and $NaNO_2$ in an ice bath with argon purging for 30 min. The solution was electrochemically deposited on the ITO surface by holding a constant potential. The Ab-1 antibody was then immobilized on the surface via the classical EDC/NHS conjugation reactions by first immersing the PPC−PBA modified surface in solution containing EDC and NHS for 1 h and then adding Ab-1 and incubating for an additional hour at 4 °C in an ice bath. After modifying the PPC−PBA Zw layer with Ab-1, the TNF-α was dropped on the surface and incubated for 1 h, followed by incubation in solution containing HRP. Here, the Ab-1 antigen serves as the biorecognition element of the immunosensor to which TNF-α binds. Once bound the enzyme-dependent current response of H_2O_2 from the HRP reaction with ferrocenemethanol creates an electron shuttle with the surface, where the resulting current response is directly correlated to the amount of TNF-α bound to the PBA component. Simultaneously the PPC component of the zwitterionic coating prevents nonspecific adsorption of biofouling components in solution.

The sandwich assay mechanism of the immunosensor reported comparable results to the ELISA test kit in whole blood with a LoD of 20 pg mL^{-1} and demonstrated selectivity against the interfering proteins HSA and hemoglobin. Electrochemical detection experiments were performed using the same sandwich assay immunosensor; however, an Au np-modified graphene oxide electrode surface was used to increase the electronic coupling (i.e., electron shuttle reaction kinetics) between the mixed zwitterionic layer and the electrode surface.[25] The Au np/GO based immunosensor provided a linear detection range of 0.1−200 pg mL^{-1} using successive SQW sweeps in phosphate buffer (pH 7.4), Figure 8. Although

https://doi.org/10.1021/acssensors.1c00390
ACS Sens. 2021, 6, 1482−1507

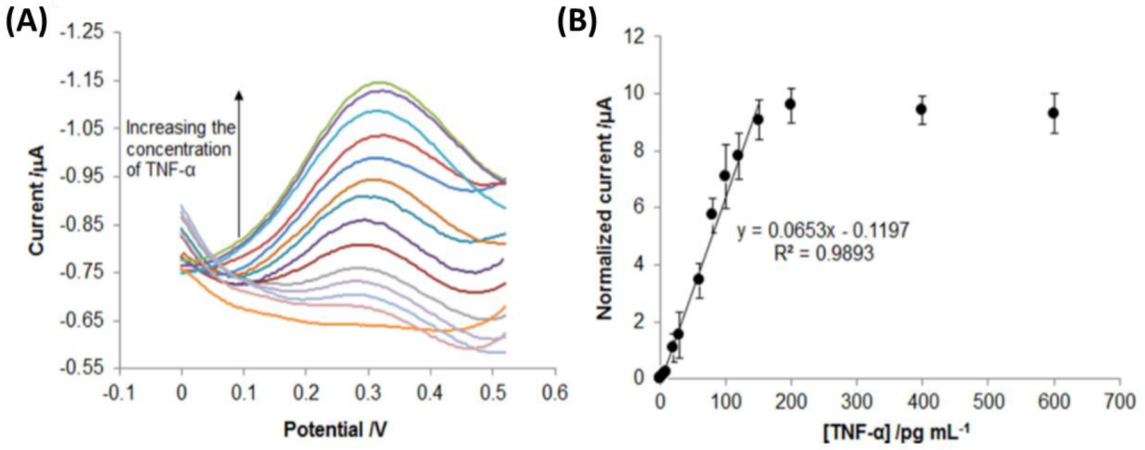

Figure 8. Electrochemical measurement results for the proposed sandwich assay immunosensor of mixed PPC−PBA Zw coatings. (A) Current (μA) vs potential (V) curves with increasing TNF-α concentration and (B) linear correlation plot of the normalized current (μA) vs the concentration of TNF-α (pg mL^{-1}). Reprinted with permission from ref 25. Copyright 2016 American Chemical Society.

good detection limits were achieved, the surface preparation steps required are lengthy and complex, involving numerous stages of incubation to create the sandwich assay. In addition, the assay requires the use of HRP and Fc to generate electrochemical detection signals rather than a direct sensing mechanism. Although valuable for stationary laboratory based biosensing applications, or some specific POC applications, the complex nature of the sandwich assay format utilized here is non-ideal for fieldwork-based POC biosensing where the target analyte to be detected may vary and direct electrochemical analysis of biological samples is required. However, the improved results with the Au/GO platform compared with ITO support the growing trend within the field of electrochemical biosensors, namely, the development of platforms which combine antifouling strategies with high-performance electrodes such as those comprised of nanoporous- or nanoparticle-based metals and/or nanocarbon-based surfaces (i.e., graphene oxide and CNTs).

The immunosensor platform based on a SAM of mixed phenyl anchored zwitterionic components shows good potential for target bioreceptor based sensing applications and has been shown to be comparable to established laboratory detection techniques such as HPLC or ELISA test kits. However, antifouling coatings based on zwitterionic polymers suffer from a major issue associated with changes in pH and surface charge, which both affect the overall charge density of the layer and give rise to strong dipole moments due to imbalances in the ionization of the individual, apposing counter charges (i.e., the loss of charge neutrality). This phenomenon has been investigated by Parvis et al., where the antifouling capabilities of Zw layers were investigated on gold substrates and were compared with previous studies of the same layers on glassy carbon.[24,34] X-ray photon spectroscopy was used to investigate the ratio of positively charged polymer amine groups (N) to negatively charged nucleic acid phosphate groups (P) of the Zw layers on each surface, otherwise known as the N/P ratio. It was found that coatings with N/P ratios closest to one (i.e., charge neutral) possessed the best antifouling capabilities, supporting the notion that charge neutrality is a property consistently associated with the prevention of protein adsorption at a surface.[88] The N/P ratio of the Zw layers on gold and glassy carbon were 0.67 and 0.93, respectively, indicating that the coatings on gold were not charge neutral, likely a result of the intrinsically high polarity of metal surfaces. This created Zw layers on gold which were less dense and less stable than those on glassy carbon. The density and stability of Zw layers was shown to be a significant and interrelated factor associated with antifouling, where charge neutral coatings with high densities provided the best antifouling performance.[132]

As a result, biosensor platform designs using Zw polymer coatings throughout literature are not typically investigated on metal surfaces with high polarities or in biological media with varying pH levels (i.e., blood, plasma, saliva, and urine) as these parameters can alter the charge density of the layer and diminish or even reverse the antifouling properties of the coating. In addition, it is important to note that most zwitterionic species are not commercially available and involve complex and lengthy synthesis techniques, making them difficult to implement for commercial manufacturing purposes. For the purpose of developing a biosensor platform for electrochemical detection in biological media for POC diagnostic applications, focus must be shifted toward a more robust strategy with respect to changes in pH and surface charge as well as commercial manufacture compatibility.

LUBRICIN

Proteoglycan 4, or lubricin, is a cytoprotective glycoprotein that is secreted in the synovial fluid of articular joints in almost all mammals and serves as a major component for boundary lubrication helping to maintain low friction between cartilage surfaces.[78,99,100,133] LUB molecules are comprised of three major domains including a long heavily glycosylated mucin domain flanked by two end-domains on either side of the protein. LUB self-assembles onto surfaces via strong covalent binding of the end-domain terminals which allows the mucin domain to orient outward toward bulk solution with a large degree of conformational freedom.

The telechelic brush structure and loop orientation of the LUB molecules once bound to the surface, as shown in Figure 9, is a crucial factor directly related to the superior antifouling characteristics exhibited by LUB coatings. Neutron reflectometry experiments in the same study using a native SiO_2 surface oxide layer demonstrated that the LUB coatings occupy just 15% of the total surface area of the substrate, revealed that the mucin domain is extremely hydrated (~95% water), and

https://doi.org/10.1021/acssensors.1c00390
ACS Sens. 2021, 6, 1482−1507

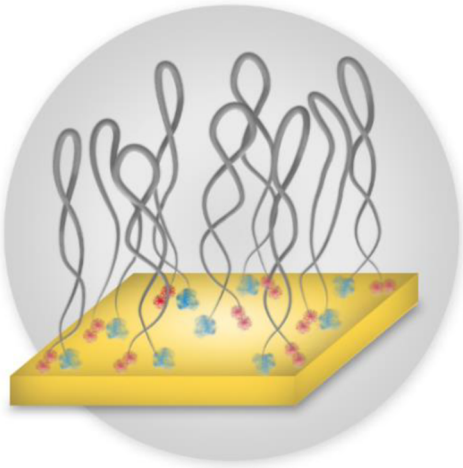

Figure 9. Illustration showing the looped orientation of LUB strands once bound to a surface, creating an overall highly dense and uniform brush coating.

found that the grafting distance between LUB molecules (~8–14 nm) is extremely large for a fully extended brush layer. The hydrophilicity of the LUB brush coatings prevent protein adsorption via a reduction in nonpolar interactions similar to traditional polymer coatings (Zws, PEG), while the molecular loop orientation of each molecule within the brush creates a large overall steric repulsion that prevents large fouling molecules from penetrating the brush layer and fouling the surface. The primary function of LUB is as a component of synovial fluid for boundary lubrication in articular joints; however, the biological composition and molecular structure of LUB coatings gives way to a plethora of advantageous characteristics including self-assembly, antiadhesive properties,[79] size-selectivity,[134] low surface coverage, and an overall negative charge via the *N*-acetylneuraminic acid (NeuAc) terminated glycan dominance within the mucin domain.[135]

Fabrication of the LUB antiadhesive coatings involves drop casting a buffer solution containing LUB on the surface and incubating for roughly 30 min to allow the self-assembly (end-anchoring via the N- and C-termini) to take place, where the grafting density of the formed LUB brush is determined by the concentration of LUB in the drop cast solution. The grafting

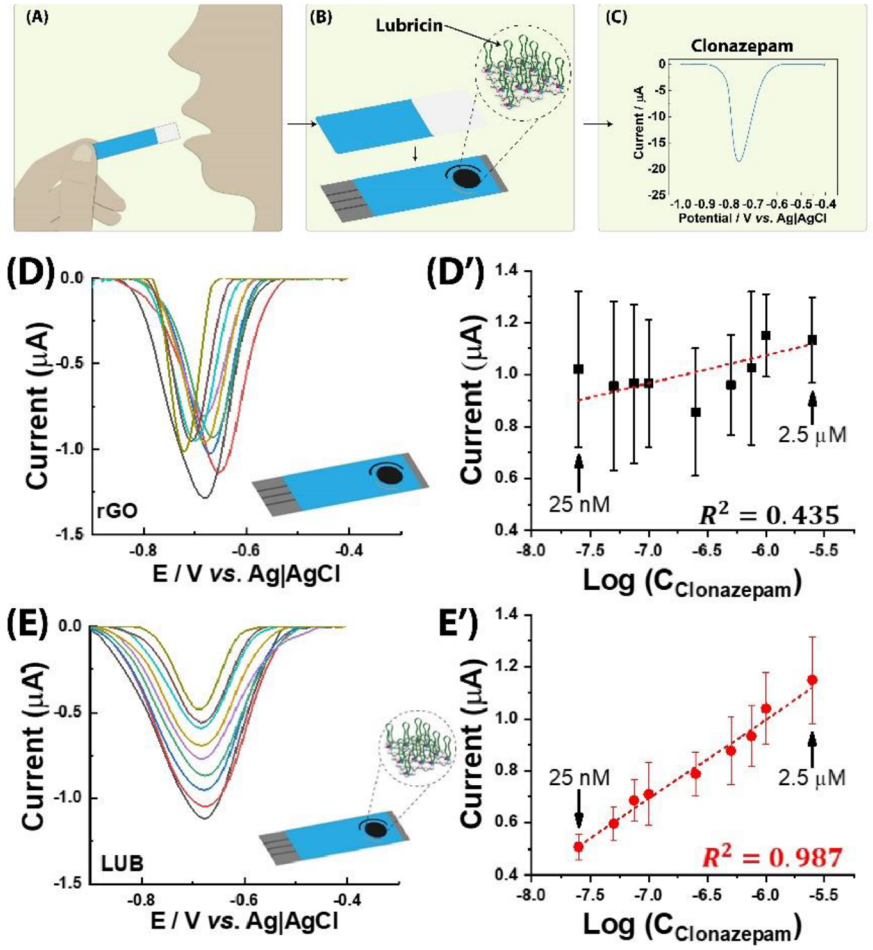

Figure 10. Schematic illustration depicting (A) saliva POC based swab sample acquisition, (B) LUB coated sensor, and (C) the resulting current profile of clonazepam derived from the electrochemical detection experiments conducted. The raw SQV data obtained for a range of clonazepam concentrations (25 nM to 2.5 μM) in unprocessed saliva samples for (D) uncoated rGO electrodes and (E) LUB coated rGO electrodes. Linear correlations were then derived from the peak current response at each concentration for the uncoated (D′) and LUB coated (E′) sensors. Error bars were established from the standard deviation of five separate SQV experiments at each concentration using a fresh sensor surface for each test. Reproduced with permissions from ref 118. Copyright 2020 WILEY-VCH Verlag GmbH & Co. KGaA, Weinheim.

https://doi.org/10.1021/acssensors.1c00390
ACS Sens. 2021, 6, 1482–1507

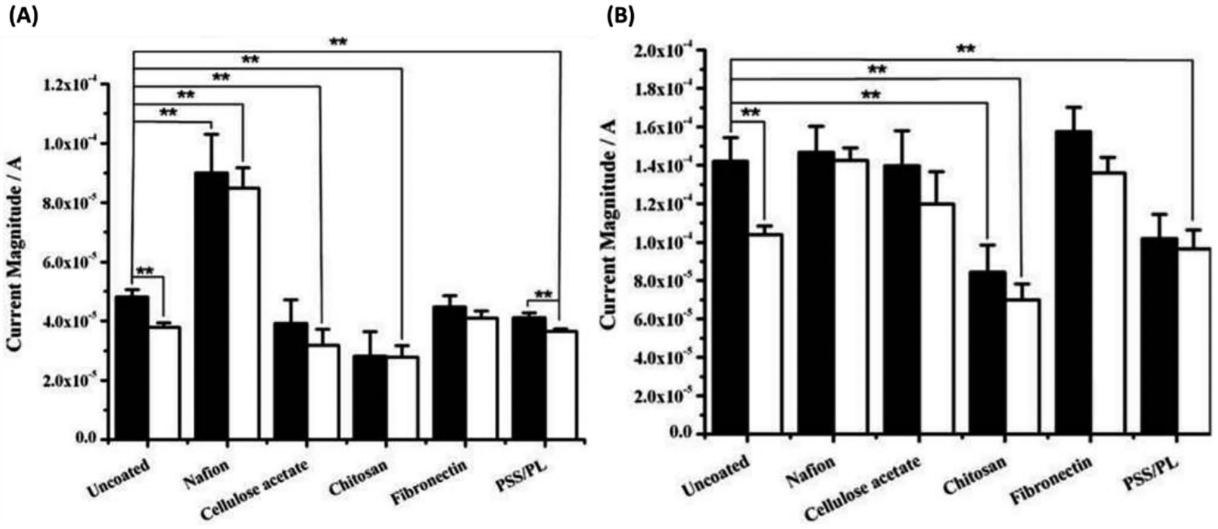

Figure 11. Current magnitudes on uncoated gold substrates and those with Nafion, cellulose acetate, chitosan, fibronectin, and PSS/PL membranes for (A) ruthenium II/III hexaammine redox couple and (B) reduction of O_2 in solutions without albumin (black) and with albumin (white). Reprinted with permission from ref 140. Copyright 2009 Elsevier.

density of the LUB coating is directly proportional to the size-selectivity; therefore, the LUB coatings can be easily tailored for a specific application via altering the concentration of LUB in the drop cast solution or shortening the adsorption period to achieve under saturated surface coverage.[136] Size-selective tailorability through a simple change in LUB concentration of the drop cast solution allows for the application of LUB antifouling coatings toward a broad range of POC biosensor based applications.

Investigations were performed for the detection of the common benzodiazepine drug Cz, or Klonopin, in unprocessed whole saliva samples.[118] A simple saliva swab sample acquisition platform was utilized with the aim toward in situ field-based electrochemical detection applications, Figure 10A–C. The combination of commercially available rGO screen-printed electrodes (SPEs) with the simple drop cast and self-assembly fabrication mechanism for the LUB antifouling coatings provided a commercially feasible and cost-effective biosensing platform.

In this study unprocessed saliva samples spiked with Cz were drop cast onto the LUB coated rGO SPEs, immediately followed by a SWV experiment in order to accurately simulate a POC saliva swab based sample acquisition and subsequent electrochemical detection method. The linear correlations obtained were derived from five individual SWV experiments (to establish error and show reproducibility) for the bare rGO SPEs and those coated with LUB to compare the antifouling and electrochemical performance of the LUB coatings respectively (Figure 10D,D′, Figure 10E,E′). The LUB coated rGO SPEs exhibited a good linear correlation (25 nM to 2.5 μM) with a LoD of 16.67 nM.[118] The five different SQV experiments run at each concentration allow for a proper analysis of the sensitivity of the system. The large error bars exhibited by the bare rGO SPE indicate a severe degree of fouling at the electrode surface and as a result, poor electrochemical sensitivity at low analyte concentrations, Figure 10D′. Therefore, it is impossible to distinguish the Cz concentration in saliva on bare rGO SPEs as the magnitude of the current responses vary significantly between experiments, Figure 10D. However, the small error bars associated with the LUB coated rGO SPE system demonstrate the effectiveness of the LUB coating at preventing nonspecific protein adsorption while simultaneously allowing the smaller Cz molecules to interact with the electrode surface, which led to excellent electrochemical sensitivity in the unprocessed saliva samples Figure 10E,E′.[118] This study highlights the advantages of combining high surface area electrodes with nonpassivating antifouling coatings for electrochemical detection in unprocessed biological media. In addition, the simple drop cast/self-assembly application method of the LUB coatings onto commercially available rGO SPEs provides a feasible and cost-effective platform toward commercial manufacture of the biosensor design.

NANOPOROUS MEMBRANES

The use of nanoporous membranes for applications in electrochemistry was pioneered in the 1980s by Baldwin et al., who first demonstrated the beneficial properties of Nafion polymer membranes on pyrolytic graphite electrodes highlighting the ease of coating application and the improved stability of the system as well as the transport properties of these membranes in a hydrogen bromide cell environement.[137,138] Nanoporous membrane based technologies have since been applied to various fields of science, including the field of biosensing due to their ability to establish a distinct and uniform physical interface between highly fouling biological media and the sensitive electrode surfaces needed for analyte detection. Nanoporous membrane technologies satisfy many of the requirements for applications in biosensing technologies (i.e., glucose sensors) including biocompatibility via nontoxic materials, stability under a range of biological conditions (i.e., pH, temperature, enzymatic activity, and protein adhesion) and commercial manufacturability with many applications.[139] Some of the common nanoporous membrane compositions investigated for physical filtration include Nafion, cellulose acetate, fibronectin, chitosan, and various polymeric mixtures. These membrane compositions were evaluated on a gold substrate to compare the respective antifouling properties and current magnitude for a ruthenium(II/III) hexaammine redox

https://doi.org/10.1021/acssensors.1c00390
ACS Sens. 2021, 6, 1482–1507

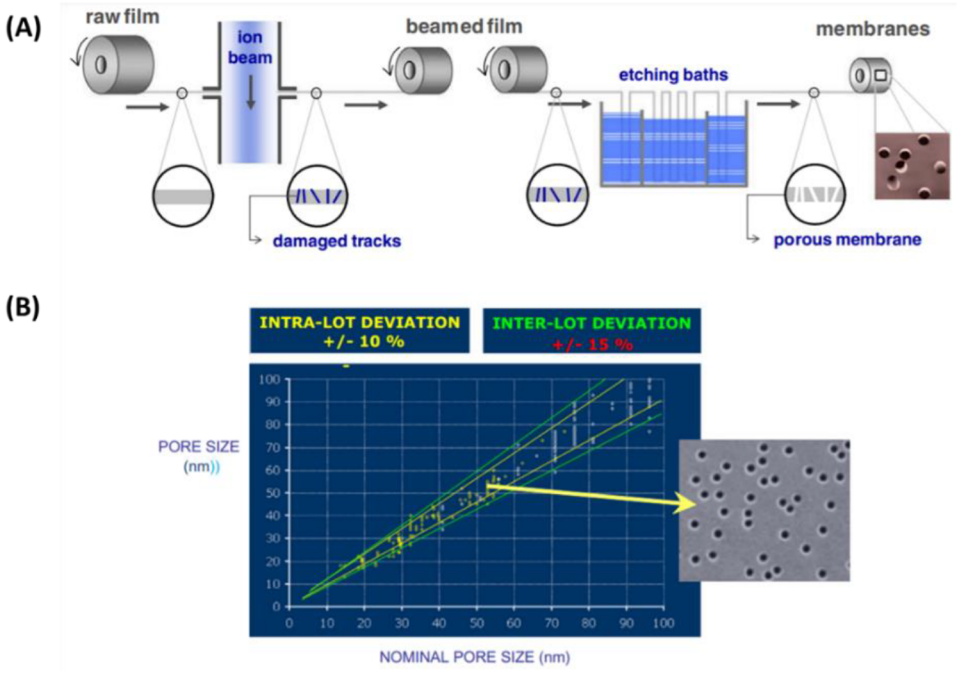

Figure 12. Schematic illustration of (A) commercially scalable ion track etching process for polymeric membranes and (B) linear correlation between the nominal and derived pore sizes. Reprinted with permission from ref 142. Copyright 2009 Elsevier.

couple and O_2 reduction in single-protein solutions of albumin, Figure 11.[140]

Several defining characteristics associated with each nanoporous membrane composition were attributed to the antifouling mechanism and resulting electrochemical signals obtained. The Nafion membrane provided a significant increase in current magnitude for the ruthenium(II/III) hexaammine redox couple. This was attributed to the affinity for cations by Nafion creating a Donnan equilibrium where the local concentration of ions within the membrane was higher than in bulk solution. This indicates that the Donnan equilibrium effect for the cations of the redox couple was able to overcome the albumin fouling associated with the observed electric double layer drop, which was not seen for the reduction of O_2. Decreased current magnitudes for both analytes were observed for the other membranes compared with bare gold and in solutions of albumin which was associated with hindered analyte diffusion, reduced electroactive surface areas, and pore clogging/surface adhesion of the albumin in solution. The comparatively large thickness of the chitosan and fibrogen membranes created a long diffusional pathway for analytes. The cellulose acetate membranes performed poorly due to large pore sizes and non-uniform pore distributions which led to pore clogging and surface fouling via albumin in solution. The intimate adsorption of the PSS−PL composite membrane to the gold surface significantly reduced the electroactive surface area, and the accumulation of albumin at the membrane surface further decreased the current magnitudes.

The different polymeric membranes investigated here are typically synthesized via solvent casting or spin coating which often create large variations of pore size and distributions (>30%) due to the lack of control over these methods, leading to the suboptimal results observed. Therefore the pursuit of more consistent membrane synthesis strategies was implemented.[141] Ion-track etching was developed to create more consistent polymeric membranes in a commercially scalable process for industrial applications, shown in Figure 12.[142]

Nanoporous polymeric membranes can be commercially produced (i.e., Millipore, Isopore) with consistent pore size distributions (~10% variation) but relatively low and randomly distributed porosities with limited pore size variability due to the nature of the polymeric film perforation mechanism via heavy metal ion beaming.[142,143] This makes ion track etched membranes good for commercial applications where specific and consistent pore sizes are suitable for a required physical filtration or separation step. However, in order to use membrane technology as an avenue toward development of antifouling biosensors, parameters such as diffusion kinetics, size-selectivity, and protein adsorption to the membrane itself must be considered; all of which are affected by the physical characteristics and composition of the membrane. Therefore a more precise degree of control over the pore size, porosity, and pore distribution is vital to the success of membranes for biosensing applications.

SILICA-BASED NANOPOROUS MEMBRANES

Microfabrication synthesis techniques such as photolithography and/or deposition/removal of sacrificial layers in silica-based materials has provided more control over the physical characteristics of the membranes.[144,145] The combination of both these microfabrication techniques has realized silica-based membranes with extremely narrow pore size distributions (>5%) and tunable pore sizes (10−100 nm range), while the silica-based composition also provides mechanical flexibility, biocompatibility, and stability in the presence of proteins and ionic solutions.[143] The realization of silica-based membranes and micromachining techniques has led to the development of mesoporous silica nanochannel membranes (SNMs). SNMs can be synthesized by reacting tetraethyl orthosilicate with a template of micellar rods which are then washed away using a solvent at the appropriate pH to create nanosized rods filled

https://doi.org/10.1021/acssensors.1c00390
ACS Sens. 2021, 6, 1482−1507

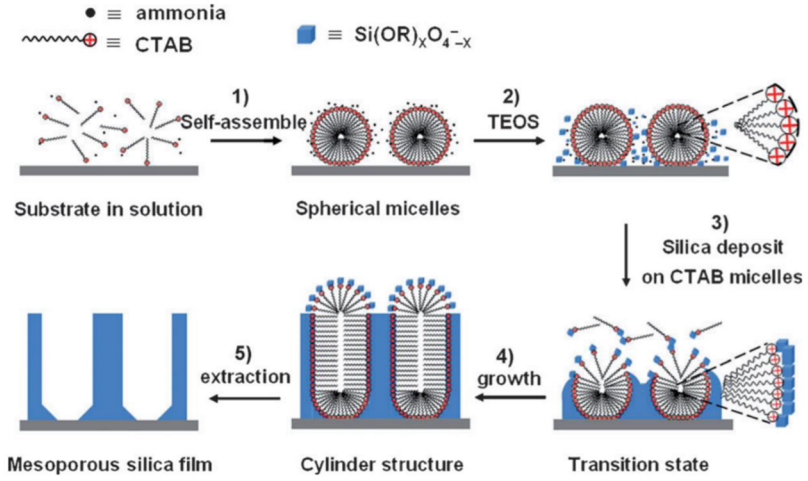

Figure 13. Schematic illustration of the Stober solution growth mechanism (SSG) used to create silica nanochannel membranes: (A) substrate in solution self-assembling into spherical micelles, (B) reaction of TEOS with the template of micellar rods, (C) silica deposited on CTAB micelles and spherical structure transitioning into a cylindrical structure, (D) growth of the cylindrical structure, and (E) extraction of the CTAB to create silica nanochannels. Reproduced with permission from ref 147. Copyright 2012 WILEY-VCH Verlag GmbH & Co. KGaA, Weinheim

with an arrangement of pores.[32,146] This technique, Stober solution growth mechanism (SSG), is the main reaction mechanism for nanoengineering silica materials, outlined in Figure 13.

Electroassisted self-assembly (EASA) is another technique often used to fabricate SNMs. This technique involves the application of a cathodic potential to an electrode immersed in a surfactant-containing hydrolyzed sol (i.e., TEOS and CTAB) solution.[148] The applied potential generates hydroxyl ions which are required in order to catalyze the polycondensation process of the precursors which self-assemble into a hexagonal packed film containing nanochannels perpendicular to the electrode surface.[149] EASA fabrication also possesses the ability to implement surface functionalization within the deposition step[150] and has been shown to produce a more ordered nanostructure with smaller pore sizes compared with the SSG mechanism for the same system (1.6 and 2.6 nm pore sizes, respectively), although the largest film thickness produced for the EASA fabricated SNMs was ∼60 nm before deposition of aggregates at the surface.[151] The recent review by Walcarius et al.[152] highlights the excellent size/charge selective sieving of SNMs, where the highly ordered nanostructure and ultrasmall pore sizes enable small positively charged molecules to permeate the nanochannels while preventing larger fouling molecules from reaching the electrode surface, demonstrating the potential for SNMs as excellent antifouling candidates for electrochemical biosensing.[153]

The antifouling ability and biological compatibility for SNMs used for electrochemical detection applications in biological fluids has been outlined in several studies and is widely agreed upon.[31,154,155] The mechanism behind the antifouling capabilities of SNMs first involves the size-selective sieving of large fouling components in solution from the target analyte via highly ordered nanochannels (up to 2.3 nm diameters). The intrinsic lypophilicity/charge selectivity of hydrophobic hydrocarbon micelle channel cores formed via the organized assembly of the cetrimonium bromide aliphatic tails during SSG synthesis of the membrane creates an environment selective for small lypophilic or neutral drugs (i.e., nonpolar compounds) and strongly prevents permeation of large, charged, and hydrophilic molecules into the membrane nanochannels. As a result, analytical sensitivity can be drastically increased via a preconcentration mechanism involving the extraction of analytes in solution by hydrophobic forces into the micelle channels prior to electrochemical detection.

The electrochemical detection of chloramphenicol, an antibiotic drug used for a variety of bacterial infections, in whole blood was performed using the SNMs grown using the SSG mechanism on an ITO substrate, Figure 14.[30] The resulting SNM possessed vertically aligned silica mesochannels highlighting geometries with 2.3 nm diameters, 111 nm thickness, and a nanochannel density of ∼4 × 10^{12} cm^{-2}.

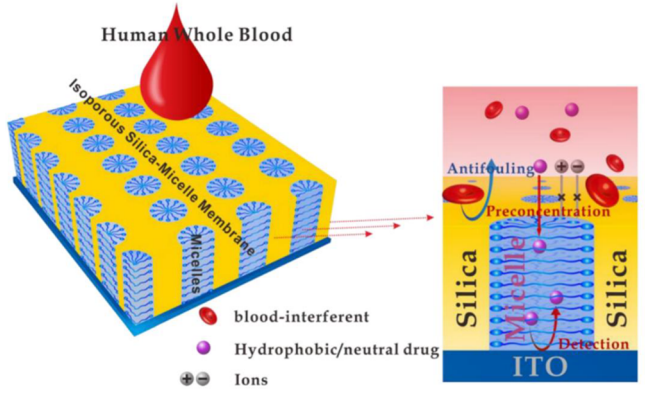

Figure 14. Illustration of the isoporous silica micelle membrane, highlighting the ability to preconcentrate hydrophobic/neutral drug compounds without any experimental steps while simultaneously preventing fouling via interferons present in whole blood samples. Reprinted with permission from ref 30. Copyright 2016 American Chemical Society

The SNM electrochemical detection system implemented in the study achieved outstanding detection of extremely low CAP concentrations in whole blood with a linear range of 0.1−3.7 ppm and an LoD of 37.7 ppb. Such low concentration detection capabilities were attributed to the intrinsic preconcentration mechanism which functionally extracts the target CAP molecules from the whole blood into the SNM

https://doi.org/10.1021/acssensors.1c00390
ACS Sens. 2021, 6, 1482−1507

channels prior to electrochemical detection without the need for any preconcentration steps. This mechanism was proved by subsequent EIS measurements showing that the micelles with hydrophobic hydrocarbon cores could effectively extract neutral lipophilic molecules from the media, where the extracted redox molecules could undergo a fast electron transfer at the micelle/ITO electrode interface.

Polymeric and biopolymer based membranes (cellulose acetate, chitosan, fibrogen, PCC/PL, and Nafion) are not ideal for applications in electrochemical detection due to hindered analyte diffusion, electrode passivation, and pore clogging from larger fouling molecules associated with non-uniformity in pore size and distribution. Silica-based membranes have good potential as they are biocompatible, have consistent pore size/distribution, and possess tunable porosity characteristics. In addition, silica is a cheap and commercially feasible material and has shown antifouling capabilities in complex samples with low concentration analyte detection. However, the SSG mechanism for silica nanochannel membranes is complex and lengthy and requires high precision to create uniform nanostructures. EASA techniques provide an improvement as the dimensions of the SNM can be easily tailored through changes in surfactant composition and the applied potential duration. The additional steps (i.e., pH adjustments using acid, several stirring/mixing steps, overnight drying/curing, and surfactant extraction) involved in the EASA fabrication technique are detailed and require user expertise to conduct properly, which can make commercial manufacture a potential challenge. In addition the nature of hydrocarbon micelle channel cores restricts SNMs to applications based on small uncharged and lypophilic analytes, although the intrinsic preconcentration mechanism due to hydrophobic force extraction of these analytes types allows detection capabilities in the parts per million range. SNMs therefore have excellent potential for POC diagnostics for specific applications orientated around specific target analyte type, and though the potential for commercial manufacture of these systems is questionable, they have shown promising performance in real/complex media.

HYDROGELS

Hydrogels are water swellable 3D structures typically comprised of polymers/biopolymers formed via physical or chemical cross-linking, exhibit beneficial properties toward antifouling applications, including biocompatibility, viscoelasticity, porosity, and compatibility with nanoparticles/bioreceptors, and possess well-known synthesis methods.[156] The material choice for each hydrogel provides a different range of properties, PVA- and PEG-based hydrogels are biocompatible and hydrophilic and have good stability in biological solutions making them common for applications such as implantable glucose sensors.[157,158] Polyacrylate hydrogels exhibit stimulus responsive (i.e., pH and temperature) reversible swelling via charged functional groups, while electroconductive hydrogels facilitate electron transfer through the structure and possess high surface area and diffusivity via porosity.[159−162] However, the primary application of hydrogels as components for electrochemical biosensing is their ability to act as transducers between the environment and the electrode surface, typically acting as a matrix for enzyme/bioreceptor immobilization, Figure 15.[163]

Bioreceptors are biorecognition molecules that exhibit specific binding with target analytes in solution and can be

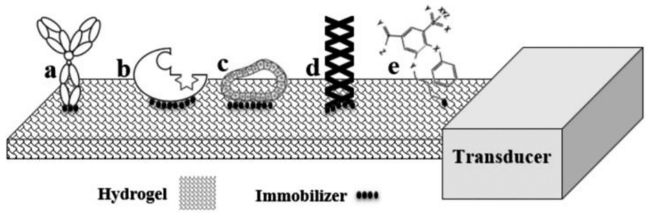

Figure 15. Diagram of five different bioreceptor types including (A) antigen/antibodies, (B) enzymes, (C) cells/cellular structures, (D) nucleic acids, and (E) biomimetic species. species. Reprinted with permission from ref 163. Copyright 2017 The Authors under Creative Commons Attribution 4.0 International license (https://creativecommons.org/licenses/by/4.0/).

organized into five categories including antigen/antibodies, enzymes, cells/cell structures, DNA, and biomimetic materials. One immobilization strategy for bioreceptors is via physical adsorption (i.e., entrapment), which is typical of hydrogels synthesized via polymerization and requires the hydrogel pores to be smaller than the bioreceptor itself in order to prevent bioreceptor leakage.[156] The most common immobilization technique however is through covalent binding between the CHO groups on polymer and the NH_2 groups on enzyme forming stable C═N bonds.[163] Although it is important to note that using covalent bonding can result in bioreceptor degradation due to limited bioreceptor release, which can lead to decreased availability and potential blockage of active bioreceptor sites contained within the hydrogel pores. Blockage of pores is a crucial phenomenon to consider for these systems as the relationship between the size of the pores, analytes, and fouling molecules as well as the bioreceptor locations within the hydrogel matrix all affect the overall electrochemical detection capabilities of the system. For a given application it is important to know the different molecules within the environment (i.e., size, conformation, and function) as well as the diffusional pathways the analytes must travel when moving toward their respective bioreceptors.

Hydrogel synthesis techniques are well-known and generally consist of dissolving monomer and initiator in solution, thorough mixing and drop casting or electrospinning the solution onto the electrode surface (poly(vinyl alcohol), sol gels, chitosan, and polyaniline).[164−170] Many polymer-based hydrogels are also electropolymerized onto the surface directly by conducting successive cycles (CVs) in solutions of sulfuric or hydrochloric acid or by application of a high constant potential.[171−173] Most hydrogel-based antifouling strategies use electrochemically active dopants including metal nanoparticles (Au, Pt, and Sn/Fe oxides) or carbon nanomaterials (CNTs, graphene, and GO) where the nanomaterial is generally dispersed in solution and is then either dropped onto the already polymerized film or mixed with the monomer/initiator solution and then drop cast onto the surface.[166,174,175] Necessary bioreceptors can then be added to the finished composite or can be incorporated into the initial solution mixture prior to deposition.

The electrochemical detection applications utilizing hydrogel-based antifouling composites investigated throughout the literature largely involve the use of a bioreceptor component for detection. While some studies have investigated various enzyme-based bioreceptor platforms such as uricase and cholesterol esterase/oxidase with enzyme immobilization via glutaraldehyde[176] or urease immobilization for the detection of

https://doi.org/10.1021/acssensors.1c00390
ACS Sens. 2021, 6, 1482−1507

urea,[177] the primary focus of hydrogel-based antifouling detection platforms are oriented toward the detection of glucose. Glucose detection involves the immobilization of glucose oxidase (GOx) via covalent binding to the hydrogel matrix where amperometric sensing can be performed through one of two electrochemical reaction mechanisms, Figure 16.[171]

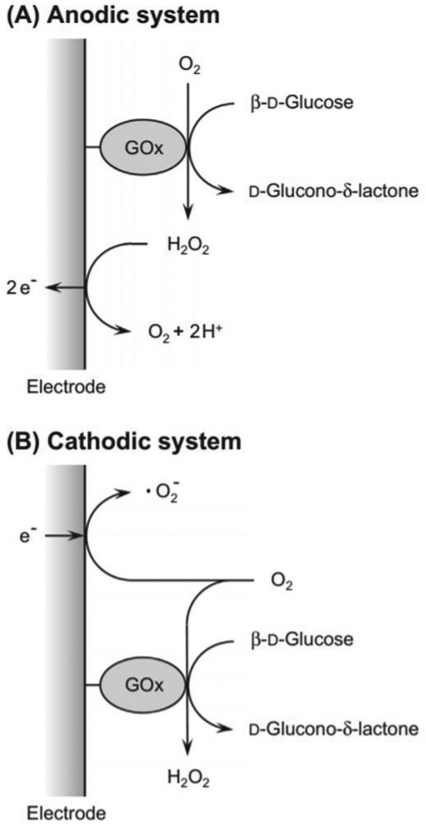

Figure 16. Diagram showing the two different reaction mechanisms for glucose detection, via amperometric detection of the decrease in O_2 concentration associated with the oxidation of glucose using (A) an anodic system and (B) a cathodic system. Reprinted with permission from ref 171. Copyright 2014 Elsevier.

The general glucose detection strategy for hydrogel-based biosensing platforms involves GOx immobilization into the hydrogel matrix, with subsequent amperometric detection of the decrease in O_2 concentration associated with glucose oxidation. However, in order to improve the electrochemical performance and antifouling capabilities of the glucose biosensing platform, many investigations include the use of different hydrogel materials and/or the addition of various components to the hydrogel matrix. The electrochemical performance of the different hydrogel platforms for glucose detection are shown in Table 3.

The synthesis techniques for creating hydrogel matrices are well-known throughout literature and the incorporation of different additives (i.e., nanomaterials) is relatively simple as no additional complicated or lengthy steps are required. Electrochemical detection using hydrogels however is based around the immobilization of enzymes and subsequent detection of specific analytes (i.e., glucose); therefore, hydrogel-based antifouling composites are not ideal for small analyte detection and are better suited for niche bioreceptor-based applications. Although many different hydrogel composites have been investigated throughout literature for these niche applications such as those in Table 3, the experiments are largely conducted in PBS solution (pH 7). Further investigation of in situ glucose detection should be conducted in biological samples in order for this technology to be realized for commercial glucose sensing applications.

Table 3. Performance of Different Hydrogel Platforms for the Detection of Glucose Including the Linear Range of Detection (mM) and the LoD (μM) for Each Composite

hydrogel composite	linear range (mM)	LoD (μM)	ref
PANi/PAA	[a]−1.1	60	171
PANi/Pt nps	0.01−8	0.7	170
PVA/Fe_3O_4 nps	0.05−2	8	165
PVA/Au nps/CNTs	0.5−8	200	166
chitosan/Au nps	0.05−2.4	2.7	172
chitosan/ferrocene/GO	0.02−6.78	7.6	164

[a]Study reports a linear increase in current response with respect to increasing concentration up to 1.1 mM but does not include the lowest concentration tested within the range.

CONCLUSIONS AND FUTURE PERSPECTIVES

This year the global coronavirus pandemic has shown the importance of developing POC-based biosensing platforms which are easy to operate with little to no training, offer rapid results, have low manufacture cost, provide highly reliable results, and can be easily deployed into the field. It was demonstrated in several countries that an effective way to reduce the spread of the virus was to combine a population quarantine with extensive testing/contact tracing.[178] This highlights how critical testing is with regard to controlling the spread of disease (i.e., detect to protect) globally; however, it also exposes many weaknesses in current biosensing technology.

POC-based electrochemical testing strategies suffer from complications primarily associated with surface fouling via the large variety of biomolecules present in the solution medium; however, they also face many manufacturing or operation protocol issues which complicate quality control and quality assurance. The issue of surface fouling on electrochemical sensors is widely established; however, the current state of antifouling sensor research trends in the direction of experimental analysis in single-protein fouling solutions (i.e., fibrogen, BSA, and IgG). Although these types of experiments can evaluate the initial reduction in fouling propensity for a given strategy, they do not establish whether the platform could be successful when testing real-world biological samples. As a result there exists an abundance of literature discussing many different types of antifouling strategies; however, very few strategies have been trending toward commercial translation. Future research into POC-based biosensors should aim to establish an experimental standard where electrochemical detection is performed in situ using clinically relevant samples without applying experimental steps that could not be easily repeated by an untrained and lightly trained operator (i.e., rinse/incubation, preconcentration, and sample pretreatment).

There exists an abundance of literature and reports on antifouling platforms for electrochemical biosensing; however, regardless of the strategy implemented, there has been very little widespread commercial success for the technology as a whole. While commercially viable antifouling strategies do exist throughout the literature, as several have been discussed here,

https://doi.org/10.1021/acssensors.1c00390
ACS Sens. 2021, 6, 1482−1507

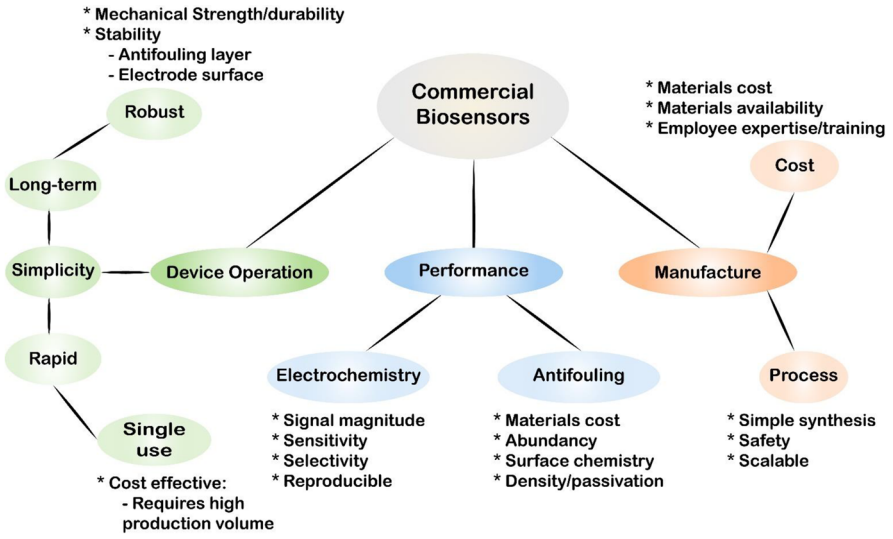

Figure 17. Diagram highlighting some of the common requirements for commercialization of electrochemical biosensors separated into three primary categories (device operation, performance, and manufacture), including the various properties of the biosensor that can be affected by each component.

it seems that no single antifouling platform has been able to meet all of the demands required for the commercial realization of a biosensing device. The flowchart shown in Figure 17 highlights many of the requirements that must be met in order to develop a commercially viable electrochemical biosensing platform, and while some of these requirements may vary with respect to the targeted application, we believe that these are some of the most common and significant hurdles to be met.

It is often true that while some technologies are successful in accomplishing one or two of the demands here, the precise mechanism which drives that success directly corresponds to its failure in another aspect of the device. As a hypothetical example, the achievement of increasingly low limits of detection in biological samples (Figure 17, performance) often requires highly complex electrode structures with ultrahigh surface areas; however, these complex electrode structures are extremely difficult to commercially manufacture having high material/manufacture costs and the various quality control checks at each stage of production, which are often required for attaining 6 sigma and/or ISO9000 standards (Figure 17, Manufacture). Antifouling coatings also suffer from commercial potential trade-offs, where many coatings provide good biofouling resistance but simultaneously cause electrode passivation at the high densities required for antiadhesion of biomolecules. In addition, commercial biosensing surfaces/electrodes developed should be compatible with user-friendly systems such as hand-held potentiostats (i.e., those used for glucose monitoring) or even the highly innovative mobile phone compatible potentiostats recently developed by Dropsens.

Consequently, we must propose the question: Can one coating meet all of the demands for commercial development? It is crucial that research within the electrochemical biosensing field pivot direction to focus on answering this question with regard to commercialization. Much of the current research within the field is oriented around the development of increasingly complex sensor platforms for ultralow limits of detection and while attaining these detection limits often captures the attention of academics and journal publishers; this hyperlimiting focus is ultimately to the detriment of the field with respect to commercial development of the technology. Many potentially viable analytes and biomarkers can be found at reasonably high concentrations (e.g., 0.1−100 uM) in bodily fluids, rendering the excess sensitivity of highly complex electrode platforms unnecessary. In most cases, the problem of electrochemical sensing in bodily fluids lies in the interference of the signal, either through excessive and unpredictable levels of "noise" or inconsistent interactions of nontarget molecules with the analyte and electrode surface, which disrupts electron transfer processes and prevents the ability to reliably correlate the electrochemical signal intensity to a specific analyte concentration. Metaphorically speaking, the academic field remains fixated on building a better high-performance sports car, while the "real world" needs a more reliable and affordable sedan to solve the problem of commercial electrochemical-based biosensing.

Better sensor platforms are therefore still required in order to combat future crises that may be similar to the pandemic we face currently. There is a dire need for biosensors that can provide chemical information on biological samples on demand, with little to no intervention from the device operator. Therefore, when developing antifouling strategies for biosensors, it is not only necessary to develop the platform but it must be evaluated in clinically relevant biological samples. It is crucial we emphasize that future investigations should challenge biosensor designs in order to gain a deeper and more thorough understanding of the underlying mechanisms behind how different antifouling strategies work and which strategies may be commercially feasible for POC based detection applications.

AUTHOR INFORMATION

Corresponding Authors

George W. Greene − *Institute for Frontier Materials and ARC Centre of Excellence for Electromaterials Science, Deakin University, Melbourne, Victoria 3216, Australia;* orcid.org/0000-0003-2250-8334; Email: wren.greene@deakin.edu.au

https://doi.org/10.1021/acssensors.1c00390
ACS Sens. 2021, 6, 1482−1507

Saimon Moraes Silva − *ARC Centre of Excellence for Electromaterials Science, Faculty of Science, Engineering and Technology, Swinburne University of Technology, Melbourne, Victoria 3122, Australia; The Aikenhead Centre for Medical Discovery, St Vincent's Hospital Melbourne, Melbourne, Victoria 3065, Australia;* orcid.org/0000-0001-6119-4417; Email: smoraessilva@swin.edu.au

Authors

Matthew J. Russo − *Institute for Frontier Materials and ARC Centre of Excellence for Electromaterials Science, Deakin University, Melbourne, Victoria 3216, Australia; The Aikenhead Centre for Medical Discovery, St Vincent's Hospital Melbourne, Melbourne, Victoria 3065, Australia*

Mingyu Han − *Institute for Frontier Materials and ARC Centre of Excellence for Electromaterials Science, Deakin University, Melbourne, Victoria 3216, Australia*

Pauline E. Desroches − *Institute for Frontier Materials and ARC Centre of Excellence for Electromaterials Science, Deakin University, Melbourne, Victoria 3216, Australia; The Aikenhead Centre for Medical Discovery, St Vincent's Hospital Melbourne, Melbourne, Victoria 3065, Australia;* orcid.org/0000-0001-7176-2246

Clayton S. Manasa − *ARC Centre of Excellence for Electromaterials Science, Faculty of Science, Engineering and Technology, Swinburne University of Technology, Melbourne, Victoria 3122, Australia; The Aikenhead Centre for Medical Discovery, St Vincent's Hospital Melbourne, Melbourne, Victoria 3065, Australia*

Jessair Dennaoui − *School of Electrical and Biomedical Engineering, RMIT University, Melbourne, Victoria 3000, Australia; The Aikenhead Centre for Medical Discovery, St Vincent's Hospital Melbourne, Melbourne, Victoria 3065, Australia*

Anita F. Quigley − *School of Electrical and Biomedical Engineering, RMIT University, Melbourne, Victoria 3000, Australia; The Aikenhead Centre for Medical Discovery, St Vincent's Hospital Melbourne, Melbourne, Victoria 3065, Australia*

Robert M. I. Kapsa − *School of Electrical and Biomedical Engineering, RMIT University, Melbourne, Victoria 3000, Australia; The Aikenhead Centre for Medical Discovery, St Vincent's Hospital Melbourne, Melbourne, Victoria 3065, Australia*

Simon E. Moulton − *ARC Centre of Excellence for Electromaterials Science, Faculty of Science, Engineering and Technology and Iverson Health Innovation Research Institute, Swinburne University of Technology, Melbourne, Victoria 3122, Australia; Centre for Regional and Rural Futures, Deakin University, Geelong, Victoria 3220, Australia;* orcid.org/0000-0002-8320-3852

Rosanne M. Guijt − *Centre for Regional and Rural Futures, Deakin University, Geelong, Victoria 3220, Australia*

Complete contact information is available at: https://pubs.acs.org/10.1021/acssensors.1c00390

Funding

Australian Research Council in the Discovery Project (DP180102287).

Notes

The authors declare no competing financial interest.

■ ACKNOWLEDGMENTS

We thank Lubris Biopharma for supporting this research through an industry funded higher degree by research scholarship and through a gift of their recombinant lubricin materials. We also acknowledge the financial support from the Australian Research Council in the Discovery Project (DP180102287) as well as the many research groups whom produced the figures used in this review article.

■ ABBREVIATIONS

BSA, bovine serum albumin; CNT, carbon nanotube; CV, cyclic voltammetry; Cz, clonazepam; DPV, differential pulse voltammetry; GO, graphene oxide; GOx, glucose oxidase; IgG, immunoglobulin G; LoD, limit of detection; LUB, lubricin; npg, nanoporous gold; PBS, phosphate buffered saline; PEG, poly(ethylene glycol); POC, point of care; SAM, self-assembled monolayer; SNM, silica nanochannel membrane; SWV, square wave voltammetry; Zw, zwitterionic

Vocabulary

Point of Care Diagnostics, biosensing platforms used for rapid analysis of biological samples taken directly from the subject (results are obtained and interpreted on-site by the device user); Electrochemical Detection, involves the sole use of electrochemical methods to detect and/or quantify specific target analytes within a sample; Nanoengineered Electrode, any fabricated electrode platform with a nanomorphology or nanostructured surface composition (i.e., typically, metal or carbon-based); Antifouling, indicates a platform which implements any strategy which serves to reduce access to or adhesion of nonspecific molecules to the sensor surface in order to maintain the electrochemical capabilities of the surface in complex media; Commercialization (Commercial Potential, Commercial Applications), translation of a research prototype into a device that can be fabricated and used commercially (this concept is frequently discussed throughout the work with regard to the various biosensor platforms presented throughout the literature; it is used to challenge and/or evaluate the potential for a given device design in terms of its viability for widespread manufacture, user operation, and electrochemical/antifouling performance with aim toward satisfying a real application within the biomedical or other related field)

■ REFERENCES

(1) Jiang, C.; Wang, G.; Hein, R.; Liu, N.; Luo, X.; Davis, J. J. Antifouling strategies for selective in vitro and in vivo sensing. *Chem. Rev.* **2020**, *120*, 3852−3889.

(2) Campuzano, S.; Pedrero, M.; Yáñez-Sedeño, P.; Pingarrón, J. M. Antifouling (bio) materials for electrochemical (bio) sensing. *Int. J. Mol. Sci.* **2019**, *20* (2), 423.

(3) Lin, P.-H.; Li, B.-R. Antifouling strategies in advanced electrochemical sensors and biosensors. *Analyst* **2020**, *145* (4), 1110−1120.

(4) Drummer, O. H. Drug testing in oral fluid. *Clin. Biochem. Rev.* **2006**, *27* (3), 147−159.

(5) Drummer, O. H. Methods for the measurement of benzodiazepines in biological samples. *J. Chromatogr., Biomed. Appl.* **1998**, *713* (1), 201−225.

(6) Vilke, G. M.; Tornabene, S. V.; Stepanski, B.; Shipp, H. E.; Upledger Ray, L.; Metz, M. A.; Vroman, D.; Anderson, M.; Murrin, P. A.; Davis, D. P.; Harley, J. Paramedic Self-Reported Medication Errors. *Prehospital Emergency Care* **2006**, *10* (4), 457−462.

(7) Yue, Z.; Molino, P. J.; Liu, X.; Wallace, G. G. J. E. C. PEGylation of platinum bio-electrodes. *Electrochem. Commun.* **2013**, *27*, 54−58.

(8) Daggumati, P.; Matharu, Z.; Wang, L.; Seker, E. J. A. C. Biofouling-resilient nanoporous gold electrodes for DNA sensing. *Anal. Chem.* **2015**, *87* (17), 8618−8622.
(9) dos Santos, W. T.; Compton, R. G. A simple method to detect the stimulant modafinil in authentic saliva using a carbon-nanotube screen-printed electrode with adsorptive stripping voltammetry. *Sens. Actuators, B* **2019**, *285*, 137−144.
(10) Hui, N.; Sun, X.; Niu, S.; Luo, X. PEGylated polyaniline nanofibers: antifouling and conducting biomaterial for electrochemical DNA sensing. *ACS Appl. Mater. Interfaces* **2017**, *9* (3), 2914−2923.
(11) Jiang, C.; Alam, M. T.; Silva, S. M.; Taufik, S.; Fan, S.; Gooding, J. J. Unique sensing interface that allows the development of an electrochemical immunosensor for the detection of tumor necrosis factor α in whole blood. *ACS sensors* **2016**, *1* (12), 1432−1438.
(12) Jiang, C.; Tanzirul Alam, M.; Parker, S. G.; Gooding, J. J. Zwitterionic Phenyl Phosphorylcholine on Indium Tin Oxide: a Low-Impedance Protein-Resistant Platform for Biosensing. *Electroanalysis* **2015**, *27* (4), 884−889.
(13) Ma, L.; Jayachandran, S.; Li, Z.; Song, Z.; Wang, W.; Luo, X. Antifouling and conducting PEDOT derivative grafted with polyglycerol for highly sensitive electrochemical protein detection in complex biological media. *J. Electroanal. Chem.* **2019**, *840*, 272−278.
(14) Prakash, V.; Sharma, S.; Kaur, J.; Mehta, S. J. A. M. Graphene oxide/lysine composite-a potent electron mediator for detection of diazepam. *Anal. Methods* **2018**, *10* (41), 5038−5046.
(15) Lozano-Chaves, M. E.; Palacios-Santander, J.; Cubillana-Aguilera, L.; Naranjo-Rodríguez, I.; Hidalgo-Hidalgo-De-Cisneros, J. J. S. Modified carbon-paste electrodes as sensors for the determination of 1, 4-benzodiazepines: application to the determination of diazepam and oxazepam in biological fluids. *Sens. Actuators, B* **2006**, *115* (2), 575−583.
(16) Habibi, B.; Jahanbakhshi, M. Silver nanoparticles/multi walled carbon nanotubes nanocomposite modified electrode: Voltammetric determination of clonazepam. *Electrochim. Acta* **2014**, *118*, 10−17.
(17) Zheng, M.; Zhou, Y.; Chen, Y.; Tang, Y.; Lu, T. Electrochemical behavior of dopamine in the presence of phosphonate and the determination of dopamine at phosphonate modified zirconia films electrode with highly antifouling capability. *Electrochim. Acta* **2010**, *55* (16), 4789−4798.
(18) Chen, T.-W.; Rajaji, U.; Chen, S.-M.; Jothi Ramalingam, R. A relative study on sonochemically synthesized mesoporous WS2 nanorods & hydrothermally synthesized WS2 nanoballs towards electrochemical sensing of psychoactive drug (Clonazepam). *Ultrason. Sonochem.* **2019**, *54*, 79−89.
(19) Veerapandian, M.; Seo, Y.-T.; Yun, K.; Lee, M.-H. Graphene oxide functionalized with silver@ silica-polyethylene glycol hybrid nanoparticles for direct electrochemical detection of quercetin. *Biosens. Bioelectron.* **2014**, *58*, 200−204.
(20) Jain, R.; Sinha, A.; Kumari, N.; Khan, A. L. A polyaniline/graphene oxide nanocomposite as a voltammetric sensor for electroanalytical detection of clonazepam. *Anal. Methods* **2016**, *8* (15), 3034−3045.
(21) Saraf, S.; Neal, C. J.; Park, S.; Das, S.; Barkam, S.; Cho, H. J.; Seal, S. J. R. A. Electrochemical study of nanoporous gold revealing anti-biofouling properties. *RSC Adv.* **2015**, *5* (58), 46501−46508.
(22) Patel, J.; Radhakrishnan, L.; Zhao, B.; Uppalapati, B.; Daniels, R. C.; Ward, K. R.; Collinson, M. M. J. A. C. Electrochemical properties of nanostructured porous gold electrodes in biofouling solutions. *Anal. Chem.* **2013**, *85* (23), 11610−11618.
(23) Cui, M.; Song, Z.; Wu, Y.; Guo, B.; Fan, X.; Luo, X. A highly sensitive biosensor for tumor maker alpha fetoprotein based on poly (ethylene glycol) doped conducting polymer PEDOT. *Biosens. Bioelectron.* **2016**, *79*, 736−741.
(24) Gui, A. L.; Luais, E.; Peterson, J. R.; Gooding, J. J. Zwitterionic phenyl layers: finally, stable, anti-biofouling coatings that do not passivate electrodes. *ACS Appl. Mater. Interfaces* **2013**, *5* (11), 4827−4835.
(25) Qi, M.; Zhang, Y.; Cao, C.; Zhang, M.; Liu, S.; Liu, G. Decoration of reduced graphene oxide nanosheets with aryldiazonium salts and gold nanoparticles toward a label-free amperometric immunosensor for detecting cytokine tumor necrosis factor-α in live cells. *Anal. Chem.* **2016**, *88* (19), 9614−9621.
(26) Liu, N.; Hui, N.; Davis, J. J.; Luo, X. Low fouling protein detection in complex biological media supported by a designed multifunctional peptide. *ACS sensors* **2018**, *3* (6), 1210−1216.
(27) Zare, M.; Tehrani, M. S.; Husain, S. W.; Azar, P. A. J. E. Multiwall Carbon Nanotube-Ionic Liquid Modified Paste Electrode as an Efficient Sensor for the Determination of Diazepam and Oxazepam in Real Samples. *Electroanalysis* **2014**, *26* (12), 2599−2606.
(28) Wang, G.; Han, R.; Su, X.; Li, Y.; Xu, G.; Luo, X. Zwitterionic peptide anchored to conducting polymer PEDOT for the development of antifouling and ultrasensitive electrochemical DNA sensor. *Biosens. Bioelectron.* **2017**, *92*, 396−401.
(29) Yang, W.; Zhang, L.; Wang, S.; White, A. D.; Jiang, S. Functionalizable and ultra stable nanoparticles coated with zwitterionic poly (carboxybetaine) in undiluted blood serum. *Biomaterials* **2009**, *30* (29), 5617−5621.
(30) Sun, Q.; Yan, F.; Yao, L.; Su, B. Anti-biofouling isoporous silica-micelle membrane enabling drug detection in human whole blood. *Anal. Chem.* **2016**, *88* (17), 8364−8368.
(31) Yan, F.; Zheng, W.; Yao, L.; Su, B. Direct electrochemical analysis in complex samples using ITO electrodes modified with permselective membranes consisting of vertically ordered silica mesochannels and micelles. *Chem. Commun.* **2015**, *51* (100), 17736−17739.
(32) Zhou, L.; Ding, H.; Yan, F.; Guo, W.; Su, B. Electrochemical detection of Alzheimer's disease related substances in biofluids by silica nanochannel membrane modified glassy carbon electrodes. *Analyst* **2018**, *143* (19), 4756−4763.
(33) Ladd, J.; Zhang, Z.; Chen, S.; Hower, J. C.; Jiang, S. Zwitterionic polymers exhibiting high resistance to nonspecific protein adsorption from human serum and plasma. *Biomacromolecules* **2008**, *9* (5), 1357−1361.
(34) Parviz, M.; Darwish, N.; Alam, M. T.; Parker, S. G.; Ciampi, S.; Gooding, J. J. Investigation of the Antifouling Properties of Phenyl Phosphorylcholine-Based Modified Gold Surfaces. *Electroanalysis* **2014**, *26* (7), 1471−1480.
(35) Chapman, C. A. R.; Chen, H.; Stamou, M.; Biener, J.; Biener, M. M.; Lein, P. J.; Seker, E. Nanoporous Gold as a Neural Interface Coating: Effects of Topography, Surface Chemistry, and Feature Size. *ACS Appl. Mater. Interfaces* **2015**, *7* (13), 7093−7100.
(36) Han, J.-H.; Boo, H.; Park, S.; Chung, T. D. Electrochemical oxidation of hydrogen peroxide at nanoporous platinum electrodes and the application to glutamate microsensor. *Electrochim. Acta* **2006**, *52* (4), 1788−1791.
(37) Hu, C.; Yang, C.; Hu, S. Hydrophobic adsorption of surfactants on water-soluble carbon nanotubes: a simple approach to improve sensitivity and antifouling capacity of carbon nanotubes-based electrochemical sensors. *Electrochem. Commun.* **2007**, *9* (1), 128−134.
(38) Patel, J.; Radhakrishnan, L.; Zhao, B.; Uppalapati, B.; Daniels, R. C.; Ward, K. R.; Collinson, M. M. Electrochemical properties of nanostructured porous gold electrodes in biofouling solutions. *Anal. Chem.* **2013**, *85* (23), 11610−11618.
(39) Jia, F.; Yu, C.; Deng, K.; Zhang, L. Nanoporous metal (Cu, Ag, Au) films with high surface area: general fabrication and preliminary electrochemical performance. *J. Phys. Chem. C* **2007**, *111* (24), 8424−8431.
(40) Daggumati, P.; Matharu, Z.; Seker, E. Effect of Nanoporous Gold Thin Film Morphology on Electrochemical DNA Sensing. *Anal. Chem.* **2015**, *87* (16), 8149−8156.
(41) Matharu, Z.; Daggumati, P.; Wang, L.; Dorofeeva, T. S.; Li, Z.; Seker, E. Nanoporous-gold-based electrode morphology libraries for investigating structure-property relationships in nucleic acid based electrochemical biosensors. *ACS Appl. Mater. Interfaces* **2017**, *9* (15), 12959−12966.

https://doi.org/10.1021/acssensors.1c00390
ACS Sens. 2021, 6, 1482−1507

(42) Kim, S. H. Nanoporous gold: preparation and applications to catalysis and sensors. *Curr. Appl. Phys.* **2018**, *18* (7), 810−818.
(43) Seker, E.; Reed, M. L.; Begley, M. R. Nanoporous gold: Fabrication, characterization, and applications. *Materials* **2009**, *2* (4), 2188−2215.
(44) Silva, T. A.; Khan, M. R. K.; Fatibello-Filho, O.; Collinson, M. M. Simultaneous electrochemical sensing of ascorbic acid and uric acid under biofouling conditions using nanoporous gold electrodes. *J. Electroanal. Chem.* **2019**, *846*, 113160.
(45) Liu, Z.; Zhang, H.; Hou, S.; Ma, H. Highly sensitive and selective electrochemical detection of L-cysteine using nanoporous gold. *Microchim. Acta* **2012**, *177* (3−4), 427−433.
(46) Fabrizius-Homan, D.; Cooper, S. A comparison of the adsorption of three adhesive proteins to biomaterial surfaces. *J. Biomater. Sci., Polym. Ed.* **1992**, *3* (1), 27−47.
(47) Sabate del Rio, J.; Henry, O. Y. F.; Jolly, P.; Ingber, D. E. An antifouling coating that enables affinity-based electrochemical biosensing in complex biological fluids. *Nat. Nanotechnol.* **2019**, *14* (12), 1143−1149.
(48) Gooding, J. J. Finally, a simple solution to biofouling. *Nat. Nanotechnol.* **2019**, *14* (12), 1089−1090.
(49) Guo, J.; Lindner, E. Cyclic Voltammograms at Coplanar and Shallow Recessed Microdisk Electrode Arrays: Guidelines for Design and Experiment. *Anal. Chem.* **2009**, *81* (1), 130−138.
(50) Kaniewska, K.; Kyriacou, K.; Donten, M.; Stojek, Z.; Karbarz, M. Micro-and nanoelectrode array behavior at regularly sized electrode modified with a thin film of thermoresponsive polymeric gel. *Electrochim. Acta* **2018**, *290*, 595−604.
(51) Rahimi-Nasrabadi, M.; Khoshroo, A.; Mazloum-Ardakani, M. J. S. Electrochemical determination of diazepam in real samples based on fullerene-functionalized carbon nanotubes/ionic liquid nanocomposite. *Sens. Actuators, B* **2017**, *240*, 125−131.
(52) Kachoosangi, R. T.; Musameh, M. M.; Abu-Yousef, I.; Yousef, J. M.; Kanan, S. M.; Xiao, L.; Davies, S. G.; Russell, A.; Compton, R. G. Carbon nanotube- ionic liquid composite sensors and biosensors. *Anal. Chem.* **2009**, *81* (1), 435−442.
(53) Shang, N. G.; Papakonstantinou, P.; McMullan, M.; Chu, M.; Stamboulis, A.; Potenza, A.; Dhesi, S. S.; Marchetto, H. Catalyst-free efficient growth, orientation and biosensing properties of multilayer graphene nanoflake films with sharp edge planes. *Adv. Funct. Mater.* **2008**, *18* (21), 3506−3514.
(54) Alwarappan, S.; Erdem, A.; Liu, C.; Li, C.-Z. Probing the electrochemical properties of graphene nanosheets for biosensing applications. *J. Phys. Chem. C* **2009**, *113* (20), 8853−8857.
(55) Wang, Y.; Li, Y.; Tang, L.; Lu, J.; Li, J. Application of graphene-modified electrode for selective detection of dopamine. *Electrochem. Commun.* **2009**, *11* (4), 889−892.
(56) Wang, Z.; Zhou, X.; Zhang, J.; Boey, F.; Zhang, H. Direct electrochemical reduction of single-layer graphene oxide and subsequent functionalization with glucose oxidase. *J. Phys. Chem. C* **2009**, *113* (32), 14071−14075.
(57) Kang, X.; Wang, J.; Wu, H.; Aksay, I. A.; Liu, J.; Lin, Y. Glucose oxidase-graphene-chitosan modified electrode for direct electrochemistry and glucose sensing. *Biosens. Bioelectron.* **2009**, *25* (4), 901−905.
(58) Zhou, M.; Zhai, Y.; Dong, S. Electrochemical sensing and biosensing platform based on chemically reduced graphene oxide. *Anal. Chem.* **2009**, *81* (14), 5603−5613.
(59) Shao, Y.; Wang, J.; Wu, H.; Liu, J.; Aksay, I. A.; Lin, Y. Graphene based electrochemical sensors and biosensors: a review. *Electroanalysis* **2010**, *22* (10), 1027−1036.
(60) Rubianes, M. A. D.; Rivas, G. A. Carbon nanotubes paste electrode. *Electrochem. Commun.* **2003**, *5* (8), 689−694.
(61) Lin, Y.; Lu, F.; Tu, Y.; Ren, Z. Glucose biosensors based on carbon nanotube nanoelectrode ensembles. *Nano Lett.* **2004**, *4* (2), 191−195.
(62) Lu, J.; Drzal, L. T.; Worden, R. M.; Lee, I. Simple fabrication of a highly sensitive glucose biosensor using enzymes immobilized in exfoliated graphite nanoplatelets nafion membrane. *Chem. Mater.* **2007**, *19* (25), 6240−6246.
(63) Huang, J.; Liu, Y.; You, T. Carbon nanofiber based electrochemical biosensors: A review. *Anal. Methods* **2010**, *2* (3), 202−211.
(64) Zhou, M.; Shang, L.; Li, B.; Huang, L.; Dong, S. Highly ordered mesoporous carbons as electrode material for the construction of electrochemical dehydrogenase-and oxidase-based biosensors. *Biosens. Bioelectron.* **2008**, *24* (3), 442−447.
(65) Smith, J. P.; Metters, J. P.; Kampouris, D. K.; Lledo-Fernandez, C.; Sutcliffe, O. B.; Banks, C. E. Forensic electrochemistry: the electroanalytical sensing of Rohypnol®(flunitrazepam) using screen-printed graphite electrodes without recourse for electrode or sample pre-treatment. *Analyst* **2013**, *138* (20), 6185−6191.
(66) Andrade, J. D. *Surface and Interfacial Aspects of Biomedical Polymers: Vol. 1 Surface Chemistry and Physics*. Springer Science & Business Media, 2012.
(67) Jeon, S.; Lee, J.; Andrade, J.; De Gennes, P. Protein—surface interactions in the presence of polyethylene oxide: I. Simplified theory. *J. Colloid Interface Sci.* **1991**, *142* (1), 149−158.
(68) Lee, J. H.; Lee, H. B.; Andrade, J. D. Blood compatibility of polyethylene oxide surfaces. *Prog. Polym. Sci.* **1995**, *20* (6), 1043−1079.
(69) Hucknall, A.; Rangarajan, S.; Chilkoti, A. In pursuit of zero: polymer brushes that resist the adsorption of proteins. *Adv. Mater.* **2009**, *21* (23), 2441−2446.
(70) Rodriguez Emmenegger, C.; Brynda, E.; Riedel, T.; Sedlakova, Z.; Houska, M.; Alles, A. B. Interaction of blood plasma with antifouling surfaces. *Langmuir* **2009**, *25* (11), 6328−6333.
(71) Binazadeh, M.; Faghihnejad, A.; Unsworth, L. D.; Zeng, H. Understanding the effect of secondary structure on molecular interactions of Poly-l-lysine with different substrates by SFA. *Biomacromolecules* **2013**, *14* (10), 3498−3508.
(72) Cao, Z.; Jiang, S. Super-hydrophilic zwitterionic poly (carboxybetaine) and amphiphilic non-ionic poly (ethylene glycol) for stealth nanoparticles. *Nano Today* **2012**, *7* (5), 404−413.
(73) Tauhardt, L.; Kempe, K.; Gottschaldt, M.; Schubert, U. S. Poly (2-oxazoline) functionalized surfaces: from modification to application. *Chem. Soc. Rev.* **2013**, *42* (20), 7998−8011.
(74) Konradi, R.; Acikgoz, C.; Textor, M. Polyoxazolines for nonfouling surface coatings—a direct comparison to the gold standard PEG. *Macromol. Rapid Commun.* **2012**, *33* (19), 1663−1676.
(75) Hoogenboom, R. Poly (2-oxazoline) s: a polymer class with numerous potential applications. *Angew. Chem., Int. Ed.* **2009**, *48* (43), 7978−7994.
(76) Sedlacek, O.; Monnery, B. D.; Filippov, S. K.; Hoogenboom, R.; Hruby, M. Poly (2-Oxazoline) s-Are They More Advantageous for Biomedical Applications Than Other Polymers? *Macromol. Rapid Commun.* **2012**, *33* (19), 1648−1662.
(77) Lowe, S.; O'Brien-Simpson, N. M.; Connal, L. A. Antibiofouling polymer interfaces: poly (ethylene glycol) and other promising candidates. *Polym. Chem.* **2015**, *6* (2), 198−212.
(78) Jay, G. D.; Harris, D. A.; Cha, C.-J. J. G. J. Boundary lubrication by lubricin is mediated by O-linked β (1−3) Gal-GalNAc oligosaccharides. *Glycoconjugate J.* **2001**, *18* (10), 807−815.
(79) Aninwene, G. E.; Abadian, P. N.; Ravi, V.; Taylor, E. N.; Hall, D. M.; Mei, A.; Jay, G. D.; Goluch, E. D.; Webster, T. J. Lubricin: A novel means to decrease bacterial adhesion and proliferation. *J. Biomed. Mater. Res., Part A* **2015**, *103* (2), 451−462.
(80) Greene, G. W.; Martin, L. L.; Tabor, R. F.; Michalczyk, A.; Ackland, L. M.; Horn, R. Lubricin: A versatile, biological anti-adhesive with properties comparable to polyethylene glycol. *Biomaterials* **2015**, *53*, 127−136.
(81) Emilsson, G.; Schoch, R. L.; Feuz, L.; Hook, F.; Lim, R. Y.; Dahlin, A. B. Strongly stretched protein resistant poly(ethylene glycol) brushes prepared by grafting-to. *ACS Appl. Mater. Interfaces* **2015**, *7* (14), 7505−7515.

https://doi.org/10.1021/acssensors.1c00390
ACS Sens. 2021, 6, 1482−1507

(82) Tang, S.; McGhie, A. Imaging individual chaperonin and immunoglobulin G molecules with scanning tunneling microscopy. *Langmuir* **1996**, *12* (4), 1088−1093.
(83) He, X. M.; Carter, D. C. Atomic structure and chemistry of human serum albumin. *Nature* **1992**, *358* (6383), 209−215.
(84) Leonard, E.; Vroman, L. Is the Vroman effect of importance in the interaction of blood with artificial materials? *J. Biomater. Sci., Polym. Ed.* **1992**, *3* (1), 95−107.
(85) Vroman, L. Finding seconds count after contact with blood (and that is all I did). *Colloids Surf., B* **2008**, *62* (1), 1−4.
(86) Rodriguez-Emmenegger, C.; Jäger, A.; Jäger, E.; Stepanek, P.; Alles, A. B.; Guterres, S.; Pohlmann, A.; Brynda, E. Polymeric nanocapsules ultra stable in complex biological media. *Colloids Surf., B* **2011**, *83* (2), 376−381.
(87) Kingshott, P.; Wei, J.; Bagge-Ravn, D.; Gadegaard, N.; Gram, L. Covalent attachment of poly (ethylene glycol) to surfaces, critical for reducing bacterial adhesion. *Langmuir* **2003**, *19* (17), 6912−6921.
(88) Ostuni, E.; Chapman, R. G.; Holmlin, R. E.; Takayama, S.; Whitesides, G. M. J. L. A survey of structure- property relationships of surfaces that resist the adsorption of protein. *Langmuir* **2001**, *17* (18), 5605−5620.
(89) Riedel, T. S.; Riedelová-Reicheltová, Z.; Májek, P.; Rodriguez-Emmenegger, C.; Houska, M.; Dyr, J. E.; Brynda, E. Complete identification of proteins responsible for human blood plasma fouling on poly (ethylene glycol)-based surfaces. *Langmuir* **2013**, *29* (10), 3388−3397.
(90) Szleifer, I. Protein adsorption on surfaces with grafted polymers: a theoretical approach. *Biophys. J.* **1997**, *72* (2), 595−612.
(91) Moyano, D. F.; Saha, K.; Prakash, G.; Yan, B.; Kong, H.; Yazdani, M.; Rotello, V. M. Fabrication of corona-free nanoparticles with tunable hydrophobicity. *ACS Nano* **2014**, *8* (7), 6748−6755.
(92) Smith, R. S.; Zhang, Z.; Bouchard, M.; Li, J.; Lapp, H. S.; Brotske, G. R.; Lucchino, D. L.; Weaver, D.; Roth, L. A.; Coury, A. Vascular catheters with a nonleaching poly-sulfobetaine surface modification reduce thrombus formation and microbial attachment. *Sci. Transl. Med.* **2012**, *4* (153), 153ra132.
(93) Cheng, G.; Li, G.; Xue, H.; Chen, S.; Bryers, J. D.; Jiang, S. Zwitterionic carboxybetaine polymer surfaces and their resistance to long-term biofilm formation. *Biomaterials* **2009**, *30* (28), 5234−5240.
(94) Yang, W.; Xue, H.; Li, W.; Zhang, J.; Jiang, S. Pursuing "zero" protein adsorption of poly (carboxybetaine) from undiluted blood serum and plasma. *Langmuir* **2009**, *25* (19), 11911−11916.
(95) Patten, T. E.; Matyjaszewski, K. Atom transfer radical polymerization and the synthesis of polymeric materials. *Adv. Mater.* **1998**, *10* (12), 901−915.
(96) Ruiz-Valdepeñas Montiel, V. C.; Sempionatto, J. R.; Esteban-Fernández de Ávila, B.; Whitworth, A.; Campuzano, S.; Pingarrón, J. M.; Wang, J. Delayed sensor activation based on transient coatings: Biofouling protection in complex biofluids. *J. Am. Chem. Soc.* **2018**, *140* (43), 14050−14053.
(97) Ruiz-Valdepenas Montiel, V.; Sempionatto, J. R.; Campuzano, S.; Pingarron, J. M.; Esteban Fernandez de Avila, B.; Wang, J. Direct electrochemical biosensing in gastrointestinal fluids. *Anal. Bioanal. Chem.* **2019**, *411* (19), 4597−4604.
(98) Ederth, T.; Lerm, M.; Orihuela, B.; Rittschof, D. Resistance of Zwitterionic Peptide Monolayers to Biofouling. *Langmuir* **2019**, *35* (5), 1818−1827.
(99) Jay, G. D.; Waller, K. A. The biology of lubricin: near frictionless joint motion. *Matrix Biol.* **2014**, *39*, 17−24.
(100) Jay, G. D. Lubricin and surfacing of articular joints. *Curr. Opin. Orthop.* **2004**, *15* (5), 355−359.
(101) Greene, G. W.; Thapa, R.; Holt, S. A.; Wang, X.; Garvey, C. J.; Tabor, R. F. Structure and Property Changes in Self-Assembled Lubricin Layers Induced by Calcium Ion Interactions. *Langmuir* **2017**, *33* (10), 2559−2570.
(102) Chen, S.; Cao, Z.; Jiang, S. Ultra-low fouling peptide surfaces derived from natural amino acids. *Biomaterials* **2009**, *30* (29), 5892−5896.
(103) Keefe, A. J.; Caldwell, K. B.; Nowinski, A. K.; White, A. D.; Thakkar, A.; Jiang, S. Screening nonspecific interactions of peptides without background interference. *Biomaterials* **2013**, *34* (8), 1871−1877.
(104) Nowinski, A. K.; Sun, F.; White, A. D.; Keefe, A. J.; Jiang, S. Sequence, structure, and function of peptide self-assembled monolayers. *J. Am. Chem. Soc.* **2012**, *134* (13), 6000−6005.
(105) White, A. D.; Nowinski, A. K.; Huang, W.; Keefe, A. J.; Sun, F.; Jiang, S. Decoding nonspecific interactions from nature. *Chemical Science* **2012**, *3* (12), 3488−3494.
(106) Liu, E. J.; Sinclair, A.; Keefe, A. J.; Nannenga, B. L.; Coyle, B. L.; Baneyx, F. O.; Jiang, S. EKylation: addition of an alternating-charge peptide stabilizes proteins. *Biomacromolecules* **2015**, *16* (10), 3357−3361.
(107) Sakala, G. P.; Reches, M. Peptide-based approaches to fight biofouling. *Adv. Mater. Interfaces* **2018**, *5* (18), 1800073.
(108) Menchicchi, B.; Hensel, A.; Goycoolea, F. M. Polysaccharides as bacterial antiadhesive agents and "smart" constituents for improved drug delivery systems against Helicobacter pylori infection. *Curr. Pharm. Des.* **2015**, *21* (33), 4888−4906.
(109) Ham, H. O.; Park, S. H.; Kurutz, J. W.; Szleifer, I. G.; Messersmith, P. B. Antifouling glycocalyx-mimetic peptoids. *J. Am. Chem. Soc.* **2013**, *135* (35), 13015−13022.
(110) Prime, K. L.; Whitesides, G. M. Self-assembled organic monolayers: model systems for studying adsorption of proteins at surfaces. *Science* **1991**, *252*, 1164−1167.
(111) Zhao, X.-M.; Wilbur, J. L.; Whitesides, G. M. Using two-stage chemical amplification to determine the density of defects in self-assembled monolayers of alkanethiolates on gold. *Langmuir* **1996**, *12* (13), 3257−3264.
(112) Nath, N.; Hyun, J.; Ma, H.; Chilkoti, A. Surface engineering strategies for control of protein and cell interactions. *Surf. Sci.* **2004**, *570* (1−2), 98−110.
(113) Tugulu, S.; Klok, H.-A. Stability and nonfouling properties of poly (poly (ethylene glycol) methacrylate) brushes under cell culture conditions. *Biomacromolecules* **2008**, *9* (3), 906−912.
(114) Stadler, V.; Kirmse, R.; Beyer, M.; Breitling, F.; Ludwig, T.; Bischoff, F. R. PEGMA/MMA copolymer graftings: generation, protein resistance, and a hydrophobic domain. *Langmuir* **2008**, *24* (15), 8151−8157.
(115) Ma, H.; Hyun, J.; Stiller, P.; Chilkoti, A. Non-fouling" oligo (ethylene glycol)-functionalized polymer brushes synthesized by surface-initiated atom transfer radical polymerization. *Adv. Mater.* **2004**, *16* (4), 338−341.
(116) Menz, B.; Knerr, R.; Göpferich, A.; Steinem, C. Impedance and QCM analysis of the protein resistance of self-assembled PEGylated alkanethiol layers on gold. *Biomaterials* **2005**, *26* (20), 4237−4243.
(117) Haustein, N.; Gutiérrez-Sanz, Ó.; Tarasov, A. Analytical Model To Describe the Effect of Polyethylene Glycol on Ionic Screening of Analyte Charges in Transistor-Based Immunosensing. *ACS Sensors* **2019**, *4* (4), 874−882.
(118) Russo, M. J.; Quigley, A. F.; Kapsa, R. M. I.; Moulton, S. E.; Guijt, R.; Silva, S. M.; Greene, G. W. A Simple Electrochemical Swab Assay for the Rapid Quantification of Clonazepam in Unprocessed Saliva Enabled by Lubricin Antifouling Coatings. *ChemElectroChem* **2020**, *7* (13), 2851−2858.
(119) Patsalos, P. N.; Zugman, M.; Lake, C.; James, A.; Ratnaraj, N.; Sander, J. W. Serum protein binding of 25 antiepileptic drugs in a routine clinical setting: A comparison of free non-protein-bound concentrations. *Epilepsia* **2017**, *58* (7), 1234−1243.
(120) Holmlin, R. E.; Chen, X.; Chapman, R. G.; Takayama, S.; Whitesides, G. M. Zwitterionic SAMs that resist nonspecific adsorption of protein from aqueous buffer. *Langmuir* **2001**, *17* (9), 2841−2850.
(121) Tegoulia, V. A.; Rao, W.; Kalambur, A. T.; Rabolt, J. F.; Cooper, S. L. Surface properties, fibrinogen adsorption, and cellular interactions of a novel phosphorylcholine-containing self-assembled monolayer on gold. *Langmuir* **2001**, *17* (14), 4396−4404.

https://doi.org/10.1021/acssensors.1c00390
ACS Sens. 2021, 6, 1482−1507

(122) Pinson, J.; Podvorica, F. Attachment of organic layers to conductive or semiconductive surfaces by reduction of diazonium salts. *Chem. Soc. Rev.* **2005**, *34* (5), 429−439.
(123) Chen, S.; Yu, F.; Yu, Q.; He, Y.; Jiang, S. Strong resistance of a thin crystalline layer of balanced charged groups to protein adsorption. *Langmuir* **2006**, *22* (19), 8186−8191.
(124) Chen, S.; Zheng, J.; Li, L.; Jiang, S. Strong resistance of phosphorylcholine self-assembled monolayers to protein adsorption: insights into nonfouling properties of zwitterionic materials. *J. Am. Chem. Soc.* **2005**, *127* (41), 14473−14478.
(125) Levicky, R.; Herne, T. M.; Tarlov, M. J.; Satija, S. K. Using self-assembly to control the structure of DNA monolayers on gold: a neutron reflectivity study. *J. Am. Chem. Soc.* **1998**, *120* (38), 9787−9792.
(126) Lao, R.; Song, S.; Wu, H.; Wang, L.; Zhang, Z.; He, L.; Fan, C. Electrochemical interrogation of DNA monolayers on gold surfaces. *Anal. Chem.* **2005**, *77* (19), 6475−6480.
(127) Keighley, S. D.; Li, P.; Estrela, P.; Migliorato, P. Optimization of DNA immobilization on gold electrodes for label-free detection by electrochemical impedance spectroscopy. *Biosens. Bioelectron.* **2008**, *23* (8), 1291−1297.
(128) Radi, A.-E.; Acero Sánchez, J. L.; Baldrich, E.; O'Sullivan, C. K. Reusable impedimetric aptasensor. *Anal. Chem.* **2005**, *77* (19), 6320−6323.
(129) Wu, J.; Campuzano, S.; Halford, C.; Haake, D. A.; Wang, J. Ternary Surface Monolayers for Ultrasensitive (Zeptomole) Amperometric Detection of Nucleic Acid Hybridization without Signal Amplification. *Anal. Chem.* **2010**, *82* (21), 8830−8837.
(130) Jolly, P.; Formisano, N.; Tkáč, J.; Kasák, P.; Frost, C. G.; Estrela, P. Label-free impedimetric aptasensor with antifouling surface chemistry: A prostate specific antigen case study. *Sens. Actuators, B* **2015**, *209*, 306−312.
(131) Belanger, D.; Pinson, J. Electrografting: a powerful method for surface modification. *Chem. Soc. Rev.* **2011**, *40* (7), 3995−4048.
(132) Chen, Q.; Ringleb, S. I.; Hulshizer, T.; An, K.-N. Identification of the testing parameters in high frequency dynamic shear measurement on agarose gels. *J. Biomech.* **2005**, *38* (4), 959−963.
(133) Schmidt, T. A.; Gastelum, N. S.; Nguyen, Q. T.; Schumacher, B. L.; Sah, R. L. J. A. Rheumatism, Boundary lubrication of articular cartilage: role of synovial fluid constituents. *Arthritis Rheum.* **2007**, *56* (3), 882−891.
(134) Greene, G. W.; Ortiz, V.; Pozo-Gonzalo, C.; Moulton, S. E.; Wang, X.; Martin, L. L.; Michalczky, A.; Howlett, P. C. Lubricin Antiadhesive Coatings Exhibit Size-Selective Transport Properties that Inhibit Biofouling of Electrode Surfaces with Minimal Loss in Electrochemical Activity. *Adv. Mater. Interfaces* **2018**, *5* (7), 1701296.
(135) Greene, G. W.; Duffy, E.; Shallan, A.; Wuethrich, A.; Paull, B. Electrokinetic properties of lubricin antiadhesive coatings in microfluidic systems. *Langmuir* **2016**, *32* (7), 1899−1908.
(136) Silva, S. M.; Quigley, A. F.; Kapsa, R. M.; Greene, G. W.; Moulton, S. E. J. C. Lubricin on Platinum Electrodes: A Low-Impedance Protein-Resistant Surface Towards Biomedical Implantation. *ChemElectroChem* **2019**, *6* (6), 1939−1943.
(137) Rubinstein, I.; Bard, A. J. Polymer films on electrodes. 4. Nafion-coated electrodes and electrogenerated chemiluminescence of surface-attached tris (2, 2′-bipyridine) ruthenium (2+). *J. Am. Chem. Soc.* **1980**, *102* (21), 6641−6642.
(138) Baldwin, R. *Electrochemical performance and transport properties of a Nafion membrane in a hydrogen-bromine cell environment*, NASA Technical Memorandum 89862; National Aeronautics and Space Administration, Cleveland, OH, USA, 1987.
(139) Scampicchio, M.; Arecchi, A.; Lawrence, N. S.; Mannino, S. Nylon nanofibrous membrane for mediated glucose biosensing. *Sens. Actuators, B* **2010**, *145* (1), 394−397.
(140) Trouillon, R.; Combs, Z.; Patel, B. A.; O'Hare, D. J. Comparative study of the effect of various electrode membranes on biofouling and electrochemical measurements. *Electrochem. Commun.* **2009**, *11* (7), 1409−1413.
(141) Dunleavy, M. Polymeric membranes. A review of applications. *Med. Device Technol.* **1996**, *7* (4), 14−21.
(142) Hanot, H.; Ferain, E. Industrial applications of ion track technology. *Nucl. Instrum. Methods Phys. Res., Sect. B* **2009**, *267* (6), 1019−1022.
(143) Desai, T. A.; Hansford, D. J.; Leoni, L.; Essenpreis, M.; Ferrari, M. J. B. Bioelectronics, Nanoporous anti-fouling silicon membranes for biosensor applications. *Biosens. Bioelectron.* **2000**, *15* (9−10), 453−462.
(144) Yang, X.; Yang, J. M.; Tai, Y.-C.; Ho, C.-M. Micromachined membrane particle filters. *Sens. Actuators, A* **1999**, *73* (1−2), 184−191.
(145) Kittilsland, G.; Stemme, G.; Nordén, B. A sub-micron particle filter in silicon. *Sens. Actuators, A* **1990**, *23* (1−3), 904−907.
(146) Trewyn, B. G.; Nieweg, J. A.; Zhao, Y.; Lin, V. S.-Y. Biocompatible mesoporous silica nanoparticles with different morphologies for animal cell membrane penetration. *Chem. Eng. J.* **2008**, *137* (1), 23−29.
(147) Teng, Z.; Zheng, G.; Dou, Y.; Li, W.; Mou, C. Y.; Zhang, X.; Asiri, A. M.; Zhao, D. J. A. C. I. E. Highly Ordered Mesoporous Silica Films with Perpendicular Mesochannels by a Simple Stober-Solution Growth Approach. *Angew. Chem., Int. Ed.* **2012**, *51* (9), 2173−2177.
(148) Walcarius, A.; Sibottier, E.; Etienne, M.; Ghanbaja, J. Electrochemically assisted self-assembly of mesoporous silica thin films. *Nat. Mater.* **2007**, *6* (8), 602−608.
(149) Goux, A.; Etienne, M.; Aubert, E.; Lecomte, C.; Ghanbaja, J.; Walcarius, A. Oriented mesoporous silica films obtained by electro-assisted self-assembly (EASA). *Chem. Mater.* **2009**, *21* (4), 731−741.
(150) Vilà, N.; Ghanbaja, J.; Aubert, E.; Walcarius, A. Electrochemically Assisted Generation of Highly Ordered Azide-Functionalized Mesoporous Silica for Oriented Hybrid Films. *Angew. Chem.* **2014**, *126* (11), 2989−2994.
(151) Robertson, C.; Beanland, R.; Boden, S. A.; Hector, A. L.; Kashtiban, R. J.; Sloan, J.; Smith, D. C.; Walcarius, A. Ordered mesoporous silica films with pores oriented perpendicular to a titanium nitride substrate. *Phys. Chem. Chem. Phys.* **2015**, *17* (6), 4763−4770.
(152) Walcarius, A. Silica-based electrochemical sensors and biosensors: recent trends. *Current Opinion in Electrochemistry* **2018**, *10*, 88−97.
(153) Vilá, N.; André, E.; Ciganda, R.; Ruiz, J.; Astruc, D.; Walcarius, A. Molecular sieving with vertically aligned mesoporous silica films and electronic wiring through isolating nanochannels. *Chem. Mater.* **2016**, *28* (8), 2511−2514.
(154) Serrano, M. B.; Despas, C.; Herzog, G.; Walcarius, A. J. E. C. Mesoporous silica thin films for molecular sieving and electrode surface protection against biofouling. *Electrochem. Commun.* **2015**, *52*, 34−36.
(155) Yao, L.; Yan, F.; Su, B. Highly ordered surfactant micelles function as the extraction matrix for direct electrochemical detection of halonitrobenzenes at the ppb level. *Analyst* **2016**, *141* (7), 2303−2307.
(156) Brahim, S.; Narinesingh, D.; Guiseppi-Elie, A. Bio-smart hydrogels: co-joined molecular recognition and signal transduction in biosensor fabrication and drug delivery. *Biosens. Bioelectron.* **2002**, *17* (11−12), 973−981.
(157) Vaddiraju, S.; Singh, H.; Burgess, D. J.; Jain, F. C.; Papadimitrakopoulos, F. Enhanced glucose sensor linearity using poly (vinyl alcohol) hydrogels. *J. Diabetes Sci. Technol.* **2009**, *3* (4), 863−874.
(158) Muñoz, E. M.; Yu, H.; Hallock, J.; Edens, R. E.; Linhardt, R. J. Poly (ethylene glycol)-based biosensor chip to study heparin-protein interactions. *Anal. Biochem.* **2005**, *343* (1), 176.
(159) Yin, M. J.; Yao, M.; Gao, S.; Zhang, A. P.; Tam, H. Y.; Wai, P. K. A. Rapid 3D patterning of poly (acrylic acid) ionic hydrogel for miniature pH sensors. *Adv. Mater.* **2016**, *28* (7), 1394−1399.
(160) Buenger, D.; Topuz, F.; Groll, J. Hydrogels in sensing applications. *Prog. Polym. Sci.* **2012**, *37* (12), 1678−1719.

https://doi.org/10.1021/acssensors.1c00390
ACS Sens. 2021, 6, 1482−1507

(161) Choudhary, M.; Brink, R.; Nandi, D.; Siwal, S.; Mallick, K. Gold nanoparticle within the polymer chain, a multi-functional composite material, for the electrochemical detection of dopamine and the hydrogen atom-mediated reduction of Rhodamine-B, a mechanistic approach. *J. Mater. Sci.* **2017**, *52* (2), 770−781.
(162) Choudhury, N.; Sampath, S.; Shukla, A. Hydrogel-polymer electrolytes for electrochemical capacitors: an overview. *Energy Environ. Sci.* **2009**, *2* (1), 55−67.
(163) Tavakoli, J.; Tang, Y. Hydrogel based sensors for biomedical applications: an updated review. *Polymers* **2017**, *9* (8), 364.
(164) Qiu, J.-D.; Huang, J.; Liang, R.-P. Nanocomposite film based on graphene oxide for high performance flexible glucose biosensor. *Sens. Actuators, B* **2011**, *160* (1), 287−294.
(165) Sanaeifar, N.; Rabiee, M.; Abdolrahim, M.; Tahriri, M.; Vashaee, D.; Tayebi, L. A novel electrochemical biosensor based on Fe3O4 nanoparticles-polyvinyl alcohol composite for sensitive detection of glucose. *Anal. Biochem.* **2017**, *519*, 19−26.
(166) Zhang, H.; Meng, Z.; Wang, Q.; Zheng, J. A novel glucose biosensor based on direct electrochemistry of glucose oxidase incorporated in biomediated gold nanoparticles-carbon nanotubes composite film. *Sens. Actuators, B* **2011**, *158* (1), 23−27.
(167) Su, X.; Wei, J.; Ren, X.; Li, L.; Meng, X.; Ren, J.; Tang, F. A new amperometric glucose biosensor based on one-step electrospun poly (vinyl alcohol)/chitosan nanofibers. *J. Biomed. Nanotechnol.* **2013**, *9* (10), 1776−1783.
(168) Wang, B.; Li, B.; Deng, Q.; Dong, S. Amperometric Glucose Biosensor Based on Sol-Gel Organic-Inorganic Hybrid Material. *Anal. Chem.* **1998**, *70* (15), 3170−3174.
(169) Salimi, A.; Compton, R. G.; Hallaj, R. Glucose biosensor prepared by glucose oxidase encapsulated sol-gel and carbon-nanotube-modified basal plane pyrolytic graphite electrode. *Anal. Biochem.* **2004**, *333* (1), 49−56.
(170) Zhai, D.; Liu, B.; Shi, Y.; Pan, L.; Wang, Y.; Li, W.; Zhang, R.; Yu, G. Highly Sensitive Glucose Sensor Based on Pt Nanoparticle/Polyaniline Hydrogel Heterostructures. *ACS Nano* **2013**, *7* (4), 3540−3546.
(171) Homma, T.; Sumita, D.; Kondo, M.; Kuwahara, T.; Shimomura, M. Amperometric glucose sensing with polyaniline/poly (acrylic acid) composite film bearing covalently-immobilized glucose oxidase: A novel method combining enzymatic glucose oxidation and cathodic O2 reduction. *J. Electroanal. Chem.* **2014**, *712*, 119−123.
(172) Luo, X.-L.; Xu, J.-J.; Du, Y.; Chen, H.-Y. A glucose biosensor based on chitosan-glucose oxidase-gold nanoparticles biocomposite formed by one-step electrodeposition. *Anal. Biochem.* **2004**, *334* (2), 284−289.
(173) Reiter, S.; Habermüller, K.; Schuhmann, W. A reagentless glucose biosensor based on glucose oxidase entrapped into osmium-complex modified polypyrrole films. *Sens. Actuators, B* **2001**, *79* (2−3), 150−156.
(174) Wu, S.; Su, F.; Dong, X.; Ma, C.; Pang, L.; Peng, D.; Wang, M.; He, L.; Zhang, Z. Development of glucose biosensors based on plasma polymerization-assisted nanocomposites of polyaniline, tin oxide, and three-dimensional reduced graphene oxide. *Appl. Surf. Sci.* **2017**, *401*, 262−270.
(175) Li, X.; Zhou, L.; Ding, J.; Sun, L.; Su, B. Platinized Silica Nanoporous Membrane Electrodes for Low-Fouling Hydrogen Peroxide Detection. *ChemElectroChem* **2020**, *7* (9), 2081−2086.
(176) Li, L.; Wang, Y.; Pan, L.; Shi, Y.; Cheng, W.; Shi, Y.; Yu, G. A nanostructured conductive hydrogels-based biosensor platform for human metabolite detection. *Nano Lett.* **2015**, *15* (2), 1146−1151.
(177) Das, J.; Sarkar, P. Enzymatic electrochemical biosensor for urea with a polyaniline grafted conducting hydrogel composite modified electrode. *RSC Adv.* **2016**, *6* (95), 92520−92533.
(178) Reis, R. F.; de Melo Quintela, B.; de Oliveira Campos, J.; Gomes, J. M.; Rocha, B. M.; Lobosco, M.; Weber dos Santos, R. Characterization of the COVID-19 pandemic and the impact of uncertainties, mitigation strategies, and underreporting of cases in South Korea, Italy, and Brazil. *Chaos, Solitons Fractals* **2020**, *136*, 109888.

https://doi.org/10.1021/acssensors.1c00390
ACS Sens. 2021, 6, 1482−1507